CHAPTER 6

SYNTHESIS, CHARACTERIZATION AND EVALUATION OF AEEA-OXYTOCIN CONJUGATES FOR NOSE TO BRAIN DELIVERY

"Everything is theoretically impossible until it is done."

- *Robert A. Heinlein*

AEEA-Oxytocin conjugation for nose to brain delivery

6.1 Background

In contemporary practice, the modification of peptides employs sophisticated techniques from medicinal chemistry, designed to not only replicate but also stabilize. The primary objectives of these modifications are to enhance biological activity of with improved selectivity, stability, and solubility [1-6].

The advancement of stabilized peptides can be realized through a diverse array of methodologies. These methods are not limited to comprehensive chemical synthesis, intricate peptide modification processes, and development of peptidomimetics. Additionally, techniques such as cyclization, modifications at backbone and side chains of peptides, and replication of structural elements like α-helices and β-sheets are crucial. Further innovations arise from recombinant technology, which enables expansion of genetic code. Another technique, PEGylation enhances solubility and half-life of therapeutic peptides. Furthermore, the development of covalent peptide drugs represents another pivotal area within this vibrant field, showcasing the continuous evolution of peptide design to meet therapeutic needs [7].

Among selected bioactives for research work, Oxytocin has very short half-life in blood circulation (4~10 min). Therefore, it was selected as a model molecule for further research. On the path of addressing bioavailability and short half-life of Oxytocin, the aim of present study was to improve retention time of Oxytocin in body along with enhancement in its permeation across BBB through conjugation of 2-(2-(2-Aminoethoxy) ethoxy) acetic acid (AEEA) with terminal cysteine of oxytocin with improved biopharmaceutical properties. The structure of AEEA-Oxytocin depicted in Figure 6.1.

6.2 Materials and Instruments

The details of materials which were used in current research work are portrayed in Table 6.1. The details of instruments used are displayed in Table 6.2.

Table 6.1: List of raw materials and chemicals used in the current research work

Items	Source
2-(2-(2-Aminoethoxy) ethoxy) acetic acid (AEEA)	Merck, USA
Trifluoroacetic acid (TFA)	Merck, USA
Fmoc-Gly-OH	Merck, USA
Fmoc-Gly-Resin	Merck, USA

Items	Source
Tetrahydrofuran	Merck, USA
Acetic anhydride & N,N-Diisopropylethylamine (DIPEA)	Merck, USA
N,N'-Diisopropylcarbodiimide (DIPC)	Merck, USA
Hydroxybenzotriazole (HOBt)	Merck, USA
25% Piperidine	Merck, USA
Methanol for HPLC	Merck, Mumbai, India
Oxytocin	Sun Pharmaceutical Industries Ltd, Ahmednagar, India
Propidium Iodide (PI) staining kit	eBioscience, USA
Sodium Hydroxide	Merck, USA
Water for Injection	Mili-Q
Water for HPLC	Merck Specialties Pvt. Ltd., Mumbai, India
BCL2, BCL2l1, CD44, FOXO1, IL-6, IL-1β, IL-10, iNOS, MMP1, and TNF-α	Cell Signaling Technologies (USA)
Triton X 100	Merck, USA
Tween 20	Merck, USA
Multimode Plate Reader	Synergy H1M Biotech
Ellman's reagent 5,5-dithiobis (2-nitrobenzoic acid) (DTNB)	Merck, USA
Thiobarbituric acid reactive substance (TBARS)	Merck, USA

Table 6.2: Details of various instruments employed during the current research work

Instruments	Make
pH meter	Mettler Toledo, India
Analytical balance	Mettler Toledo, India
HPLC, Waters Alliance 2695	Waters, USA
NMR	Bruker DPX-300 MHz, HD-300, and HD-400 spectrometers, Germany
IR Spectrometer	Shimadzu Corporation, Japan
HRMS	Thermo Scientific, Q Exactive plus, US
Freeze Dryer, SNL216V-230	Thermo Electron (Thermo Sawant), USA
Freeze Dryer, Alpha 2-4 LD Plus	Martin Christ GmbH, Germany
FTIR, RX-100	Perkin Elmer, U.S.A.

6.3 Synthesis and Characterization of AEEA-Oxytocin

6.3.1 Synthesis of AEEA-Oxytocin

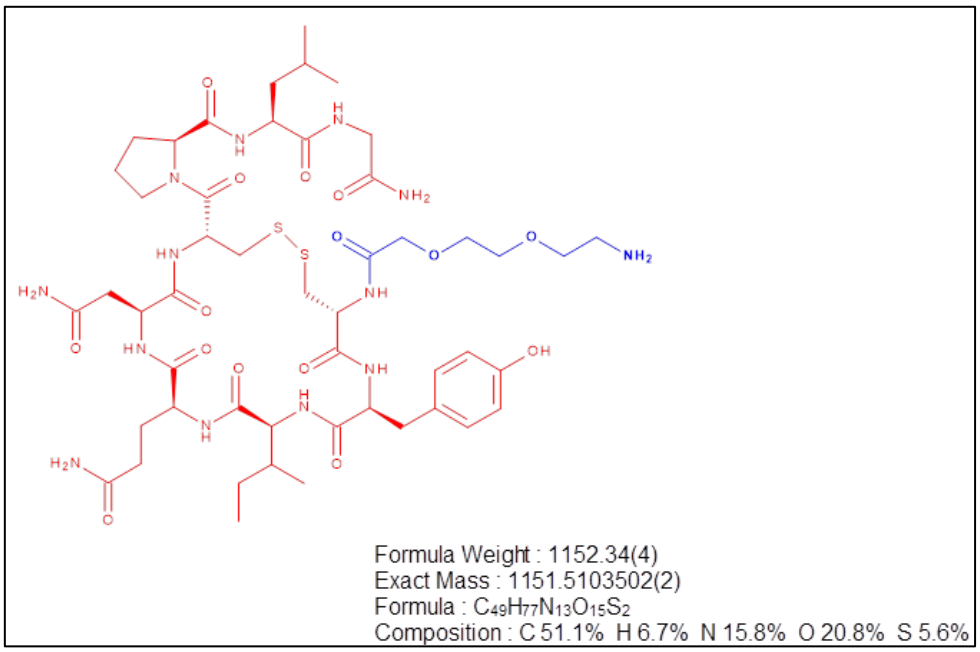

Figure 6.1: Structure of prepared AEEA-oxytocin conjugate

Sequence: AEEA-Cys-Tyr-Ile-Gln-Asn-Cys-Pro-Leu-Gly-NH2 (2-7)-disulfide

Chemical Name: AEEA-L-cysteinyl-L-tyrosyl-L-isoleucyl-L-glutaminyl-L-asparagyl-L-cysteinyl-L-prolyl-Lleucyl-glycin (2-7)-disulfide

Stage–I: Manufacture of AEEA-OXT-Stage-H-(01-10)-Resin: Fmoc-Rink amide AM resin was used as solid support for the synthesis of OXT-Stage-H-(01-09)- Resin (Figure 6.2)**.** Fmoc protection was removed by using 25% piperidine/DMF. Fmoc-Gly-OH was attached to the H-Rink amide AM Resin using Diisopropyl carbodiimide and HOBt to generate in-situ intermediate Fmoc-Gly-Resin. Selective de-blocking of Fmoc group followed by the attachment of second amino acid (Fmoc-Leu-OH) using DIPC/HOBt at 20-25°C and Tetrahydrofuran as a coupling solvent gives Fmoc-2PP (08-09)-RESIN. Acetic anhydride and Diisopropylethylamine were used to terminate the uncoupled amino groups after coupling of every amino acid. Rest of 7 amino acids were attached using DIPC/HOBt to synthesise Fmoc-(01-09)-RESIN. Finally, Fmoc group was removed using 25% piperidine/DMF to further conjugation of Fmoc-AEEA-OH performd as per Cycle 2 and followed by deblocking to remove Fmoc-protection to get modified OXT on solid support [12].

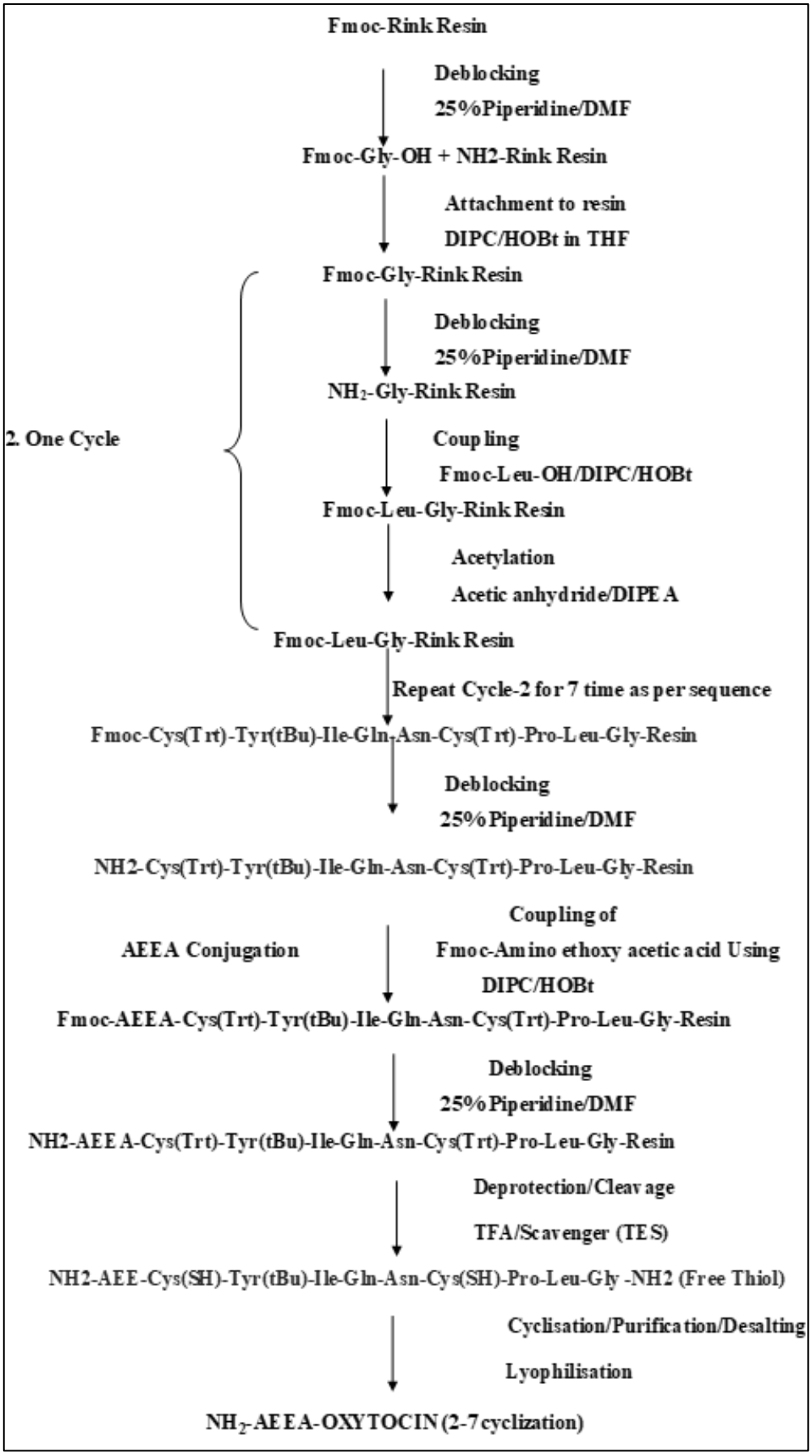

Figure 6.2: Schematic presentation of synthesis of NH_2-AEEA-OXYTOCIN

Stage–II: Manufacture of AEEA-OXT: The concluding step of process involves cleavage and removal of protective group from AEEA-OXT solids, specifically during an intermediate stage of synthesis. To accomplish this deprotection, Trifluoroacetic acid (TFA) was utilized as both cleavage and de-protection reagent, while Triethyl silane served as a scavenger agent. This combination facilitate transformation of intermediate into a crude form of AEEA-OXT free thiol [12].

Following an initial transformation, the crude product was solubilized and subjected to a cyclization reaction using iodine solution. This step was crucial for achieving the desired molecular structure. Once cyclization was complete, the mixture underwent purification to isolate final compound. The purification process employed a C-18 column, utilizing a sophisticated mobile phase that combined 0.1% TFA in acetonitrile (ACN) with 0.1% TFA in water. A gradient method was implemented, where proportion of acetonitrile was gradually increased from 10% to 30% over the course of 300 minutes, ensuring efficient separation of desired product.

After successful purification, the final step involved desalting of solution. This was achieved by introducing a 50% acetonitrile solution, containing 1% acetic acid in water, effectively removing any remaining salts and impurities. Ultimately, the purified solution was lyophilized (Freeze Dryer, Alpha 2-4 LD Plus, Martin Christ GmbH, Germany), resulting in a dry form of AEEA-OXT, as illustrated in Figure 6.2. This final product is crucial for further applications and studies [12].

6.3.2 Characterization

FTIR analysis was conducted to elucidate the functional groups present in both oxytocin and AEEA-oxytocin, as well as to investigate any potential interactions between oxytocin (OXT) and aminoethylethanolamine (AEEA). The process involved obtaining FTIR spectra for pure oxytocin and modified AEEA-oxytocin to observe any alterations in functional groups that occurred during conjugation process with AEEA. For this analysis, approximately 10-15 mg of each sample was finely mixed with potassium bromide (KBr) to form a transparent pellet. This pellet was then analyzed using a Perkin Elmer Spectrum (Version 10.03.08) spectrometer, which was carefully calibrated and operated over a resolution range of 400 to 4000 cm^{-1}.

In addition to FTIR, further characterization was achieved through the use of a Bruker NMR spectrometer. The samples were prepared with deuterated solvents, specifically

deuterium oxide (D_2O), to ensure accurate chemical shift measurements. The chemical shifts obtained were expressed in parts per million (ppm) relative to residual peaks of deuterated solvent. D_2O based NMR spectra were recorded for both unreacted oxytocin and resulting products from reaction with butyraldehyde at a temperature of 298 K. This analysis utilized a Bruker Avance III 600 NMR spectrometer, which operates at a frequency of 500.13 MHz specifically for nuclei of hydrogen (1H). The reaction mixture included 15 mg of sample suspended in 0.6 mL of D_2O, meticulously prepared to maintain field frequency stabilization during analysis. The mass of the conjugated molecule was further confirmed by a direct mass method using HRMS (Thermo Scientific, Q Exactive plus). Xcaliber software *Ver.* 4.4.16.44 was used to interpret data. The sample was prepared by dissolving AEEA-Oxytocin to get a 1000 ppm concentration. 10 µL was injected into the instrument.

6.4 *In vitro* cell line study

6.4.1 Evaluation on SH-SY5Y neuro cells

6.4.1.1 % Cell viability and biocompatibility

The assessment of cell viability was performed using MTT assay, a widely recognized method detailed in established protocols [9, 10]. This assay was specifically utilized to evaluate the biocompatibility of various formulations on neurogenic cells. For this investigation, SH-SY5Y cells were plated in 96-well at density of $5x10^3$ cells per well. The cells were then subjected to treatments with Oxytocin and AEEA-Oxytocin (1, 10, 100 µg/mL), while control group received phosphate-buffered saline (PBS) to establish a baseline. Following treatment application, the cells were allowed to incubate for varying durations of 24, 48, and 72 hours to enable sufficient interaction between formulations and cells. After the designated incubation periods, 20 µL of MTT solution (at a concentration of 5 mg/mL) was carefully added to each well. The wells were then rinsed with PBS buffered to a neutral pH of 7.4 to remove any unbound agents.

Subsequently, the plates underwent a four-hour incubation period to allow metabolically active cells to convert MTT into purple formazan crystals. Once this crystallization process was completed, 100 µL of dimethyl sulfoxide (DMSO) was added to each well to dissolve the formazan crystals, allowing for quantification. The concentration of dissolved formazan was measured using a multimode reader (Agilent, Biotek, US), set to a wavelength of 570

nm to capture absorbance of each well accurately. The readings obtained from treated wells were compared against those of PBS-treated control wells, which provided a reference point for 100% cell viability. Additionally, PBS at pH 7.4 was used as a positive control, while Triton X-100 served as the negative control, allowing for comprehensive evaluation of cell viability across the different treatments [11].

6.4.1.2 *In vitro* cell permeation study: Quantitative

In the current investigation, cellular uptake of Oxytocin (OXT) and its derivative AEEA-OXT was measured, focusing on influences of both time and concentration. This was achieved using a direct High-Performance Liquid Chromatography (HPLC) method. SH-SY5Y neuronal cells were employed for maintaining a population density of $5x10^3$ cells per well, incubated in fresh culture medium infused with varying concentrations of free Oxytocin and AEEA-OXT. These incubations were carried out over different time intervals to elucidate how both concentration and duration affect the uptake of these compounds by the cells. To quantify the percentage of cellular uptake in SH-SY5Y cells, direct exposure of the cells to different concentrations specifically, 0.1, 0.2, 0.3, and 0.4 mg of both free Oxytocin and AEEA-Oxytocin, corresponding to equivalent doses of 0.1, 0.2, 0.3, and 0.4 mg of OXT. Each set of exposures lasted for either 1 hour, 2 hours, or 3 hours, facilitating a comprehensive analysis of time-dependent uptake. Following these incubation periods, careful removal of medium to eliminate any remaining extracellular compounds. The cells were then rinsed twice with PBS at a pH of 7.4 to ensure thorough cleansing. To disrupt the cells and release internalized compounds, 0.1% Triton X-100 was employed. The extraction process involved mixing cell lysate with acetate buffer at pH 4.0 and methanol in a 1:2 ratio, effectively solubilizing internalized Oxytocin and AEEA-OXT.

Subsequently, the cell lysate was subjected to centrifugation using a Sigma K 300 centrifuge at high speed of 25,000 rpm for a duration of 30 minutes. This process allowed for the separation of the supernatant, which was then analyzed through HPLC. This analysis provided a precise quantification of internalized OXT and AEEA-OXT, enabling to gain valuable insights into their cellular uptake mechanisms [12].

6.4.1.3 Cell permeation study (Cell uptake)

Qualitatively cell uptake study was performed as method mentioned in previously published reports [9-11]. In brief, SH-SY5Y cells with $1x10^5$ population were used to assess the intracellular localization of coumarin-6 (C-6), C-6+Oxytocin and C-6+AEEA-

oxytocin. A 6-well plate was meticulously arranged, with each well containing 50,000 SH-SY5Y neuroblastoma cells, and incubated in an incubator with 5% CO_2 at 37ºC for overnight to allow the cells to firmly adhere on plate surface. The following day, adherent cells were carefully treated with C-6, C-6+OXT and C-6+AEEA-Oxytocin, at a concentration of 4 µg/mL, equivalent to C-6, for a duration of 4 hours at a controlled temperature of 37ºC. After the treatment period, cells underwent a thorough washing procedure, receiving five washes with 1X HBSS to effectively remove any excess fluorescent dye and uninternalized OXT and AEEA-OXT. To preserve cellular structure for imaging, the cells were then fixed with a 4% paraformaldehyde solution and subsequently examined under a fluorescence microscopy (NIKON-Ti2, US) using a green filter.

6.4.1.4 Cell apoptosis assay

Acridine orange (AO) and ethidium bromide (EB) dyes serve as crucial tools for visualizing extent of nuclear alterations and formation of apoptotic bodies, which are hallmark features of apoptosis in cells. AO is a cationic dye known for its ability to penetrate the intact membranes of both viable and non-viable cells, resulting in a bright green fluorescence that indicates the presence of live cells. In contrast, ethidium bromide selectively infiltrates cells with disrupted membrane integrity, a significant marker of the apoptotic process, emitting a striking red fluorescence to highlight compromised cells.

To conduct the experiment, a 12-well plate was meticulously prepared and inoculated with SH-SY5Y neuroblastoma cells, cultured at a density of 1×10^5 cells per well, and incubated for a period of 24 hours to allow for cell attachment and growth. Following this incubation phase, the seeded cells were subjected to treatment with 100 µg/mL of oxytocin and AEEA-Oxytocin, representing a higher concentration to assess their effects on cellular behaviour. After an additional incubation period of 48 hours, the treated cells underwent a thorough washing process, being rinsed three times with sterile PBS maintained at pH 7.4. Subsequently, 0.2 mM of AO and 1 mM of EB were introduced into each well, facilitating qualitative evaluation of apoptosis in treated cells. Finally, images of fluorescently stained cells were captured with aid of a fluorescence microscope, set at a magnification of 20X, allowing for detailed visualization of apoptotic changes that occurred.

6.4.1.5 Reactive Oxygen Species (ROS) Assay

ROS are molecules that interact with one or more free electrons that are generated when oxygen is reduced. Strong chemotherapeutics cause overproduction of ROS, which oxidizes DNA, lipids, and tissue proteins. This can cause problems with cell channelling, redox control, apoptosis, and cell death. This is DCFDA, a green fluorescent dye i.e., cationic and lipophilic. It is used to describe ROS that are made in cells. In cells, esterases break down DCFDA into DCF (2′7′-dichlorofluorescein), which then mixes with ROS to give off green fluorescence. To sum up, 1×10^5 SH-SY5Y cells were put into each well of a 12-well plate and left there for 24 hours. Oxytocin and AEEA-Oxytocin (100 µg/mL) were put on the plate that had seeds on top of it. Three times, PBS pH 7.4 was used to wash the cells. Then, 1 µL of diluted DCFDA (1 mg/mL) was added to each well, and cells were left to settle for 30 minutes. The cells were studied with a fluorescent microscope that had a green screen with 20X magnification.

6.4.2 Evaluation on monocytic cells (THP-1)

6.4.2.1 Analysis using genomic microarrays (qRT-PCR)

Genomic microarray (qRT-PCR) analysis in Human THP-1 cells were done as mentioned in previous chapter section 5.3.6.2.1. The mRNA expression was quantified by the changes in threshold method ($\Delta\Delta C_T$) and normalized to the house keeping ACTB mRNA (encoding β actin) expression [11, 12, 13].

6.4.2.2 Immunofluorescence assay (IFA)

The method of IFA assay for Oxytocin and AEEA-OXT in Human THP-I cells was done as mentioned in previous chapter section 5.3.6.2.2. The cells that were stained with the antibody were transferred onto slides, cleaned, and mounted using an anti-fade medium with DAPI from Thermo Fisher Scientific, USA. The images were captured using Nikon confocal microscope and data was processed and quantified by the software, Image J-Win64 [11].

6.5 Neurological activities in experimental animals

6.5.1 Methodology for Pharmacodynamics studies

While *In vitro* assessments of drug release and targeting are crucial, neurological disorders are multifactorial, complex diseases involving many physiological processes [14-18]. For instance, it is difficult to evaluate neuropsychiatric illnesses, neurodevelopmental

disorders, and epilepsy using *In vitro* models. For this reason, it is important to examine both ability of oxytocin and AEEA-Oxytocin to successfully deliver therapeutics to brain and resulting effects on disease symptoms and pathology in animal models of neurological and neuropsychiatric disease [16-19]. Methodology for Pharmacodynamics studies. Male Balb/C mice weighing 25–40 g (8–10 weeks old) were selected as the subjects for *In vivo* tests for this purpose. The mice were kept in groups of six in a controlled humidity and temperature environment. Animals were provided access of food and water *ad libitum* according to Laboratory Rodent Diet protocol approved by Institutional committee. Lights of mice housed rooms were switched on at 6 a.m. every morning and switched off at 6 p.m. to maintain 12hr light/dark cycle. All experimental treatments, gene expression research, brain hippocampus studies, and cognitive function evaluations were carried out. The National Institute of Occupational Health (NIOH), Ahmedabad's Institutional Animal Ethical Committee reviewed and approved the methods used to treat all of the study's animals (No.: *IAEC-ICMR-NIOH/2022-23/29/02/M*).

6.5.2 Morris water maze (MWM) test

In a detailed pharmacodynamic study, the effects of AEEA-oxytocin delivered via intranasal administration were compared to those of a free oxytocin (OXT) solution also administered intranasally, utilizing the Morris Water Maze (MWM) test as primary experimental design [13–15]. The study involved a rigorous four-day training trial during which mice learned to navigate to a concealed platform situated in fourth quadrant of maze, a critical element of test. After the completion of this training phase, a final acquisition trial was conducted to assess outcomes following treatment.

Throughout MWM test, parameters were measured, including time taken for the mice to locate the hidden platform and the duration spent in fourth quadrant [15]. The ability of mice to retain memory was evidenced by their reduced time to reach platform, suggesting strong memory retention capabilities. Conversely, a diminished amount of time spent in fourth quadrant indicated potential memory impairment. Control groups included a naive group and one treated with Scopolamine (SCP) via IP route, which were utilized as benchmarks for comparison. In MWM test, key factors monitored included both times taken to reach the hidden platform and time spent in fourth quadrant [14]. A shorter duration taken to locate platform suggested better memory retention integrity, while increased time in quadrant four was associated with memory decline. The study made direct comparisons

between treatments, examining groups that received SCP+oxytocin (100 µg oxytocin) and SCP + AEEA-Oxytocin (equivalent to 100 µg oxytocin) against both a positive control group (naive) and a negative control group (SCP treated).

6.5.3 Brain Hippocampus histopathological evaluation

The effectiveness of formulations proposed in this research study was evaluated through a histological assessment of hippocampus histopathological evaluation. Enhanced treatment outcomes were associated with an increased neuronal density. As previously described, the mice were euthanized following completion of treatment and data acquisition. After extraction, the brains were immersed in a fresh formaldehyde solution for a period of 24 hours. The subsequent dehydration process involved the use of ethanol, beginning with a concentration of 70% for 24 hours, followed by 90% for one hour, and concluding with 100% for an additional hour. The samples were then rinsed in xylene before being embedded in paraffin. A microtome was utilized to produce coronal sections with a thickness of 5 µm. These sections were then mounted onto glass slides and subjected to staining utilizing standard hematoxylin and eosin technique [15].

6.5.4 Gene Expression and Biochemical Studies

To verify molecular efficacy of treatment mentioned above, gene expression studies were must. The examination of gene expression in brain homogenate samples, focused on interleukin-6 (IL-6), nuclear factor erythroid 2 (Nrf2), allograft inflammatory factor 1 (AIF-1), brain-derived neurotrophic factor (BDNF), and glial fibrillary acidic protein (GFAP) analysis [17,18, 22].

The sagittal entire section of each mouse's brain was used for gene expression analysis. Total RNA from collected brain tissues was extracted using the Trizol reagent. At initial stage, quality and purity assessment of extracted RNA was conducted in order to ensure proper downstream processing. 1000 ng of total RNA was transformed into a cDNA for amplification employing a cDNA synthesis kit followed manufacturer's instructions. These tissues were subjected to qRT-PCR-based relative gene expressions for a variety of genes using SYBR green dye and the proper primers (Table 6.3). The qRT-PCR procedure involved 40 cycles, alternating between 95°C and 60°C, each lasting one minute. Data were analysed using the $2^{-\Delta\Delta Ct}$ method and values are expressed as fold change relative to the control group [17-19].

Table 6.3: Primers of Genes for qRT-PCR with their role in brain

Gene	Role	Forward (5′–3′)	Reverse (5′–3′)
AIF-1 (Allograft inflammatory factor 1)	Prominent neurodegeneration marker linked to calcium binding adaptor molecule-1	TCCGAGGAGACG TTCAGCTA	CGTGTGACATCCACCTC CAA
S100B	Cytosolic calcium-binding protein concentrated in astrocytes, is released following astroglia injury	GCGAATGTGACT TCCAGGAA	GCTTCCTAATTAGCTAC AAC
BDNF (brain-derived neurotrophic factor)	Explains antioxidant and cholinergic transmission	CGGCGCCCATGA AAGAAGTA	TCGTTGGGCCGAACCTT CT
GFAP (glial fibrillary acidic protein)	Linkage with amyloid theory and its neuroinflammation	GTGCAGAGATGA TGGAGCTC	ACTGTTGGCCGTAAGCT GGT

6.5.5 Biochemical analysis

Biochemical analysis of the brain homogenate samples of mice was done as mentioned in previous chapter 5.3.7.5. Glutathione, Malondialdehyde, Reactive Oxygen Species (ROS) and Nitrite Content was estimated for biochemical analysis [18].

6.5.6 Statistical Analysis

Statistical analyses were conducted to identify significant differences among the various experimental groups using Prism software (version 9, GraphPad). Specifically, a two-way ANOVA was employed, along with multiple comparisons, to assess several key metrics, including cell viability, uptake levels, gene transcription, expression levels, and biochemical parameters. The significance of the results was categorized as follows: **** indicates highly significant differences ($P \leq 0.0001$), *** indicates moderately significant differences ($P \leq 0.005$), ** denotes significant differences ($P \leq 0.001$), and * reflects less significant differences ($P \leq 0.05$)..

6.6 Results and discussion

6.6.1 Synthesis and characterization of AEEA-Oxytocin

The conjugation of AEEA with oxytocin was investigated using FT-IR spectroscopy in order to determine C-C band formation confirmation in AEEA-oxytocin. Spectral output

was recorded by the transmittance as a function of wave number. Additional -C-O- stretching band (1050-1150 cm^{-1}) was observed (Figure 6.3) compared to plain oxytocin IR spectra which confirms the conjugation between oxytocin and AEEA in AEEA-Oxytocin molecule [12].

Table 6.4: Observations from NMR spectra of Oxytocin

S. No.	Chemical Shift ppm	No. of Proton	Assignment of Proton	Remarks
1	0.81-0.99	12	CH_3	Isoleucine/Leucine
2	1.19-1.61	2	CH	Isoleucine/Leucine
3	1.62-3.77	22	CH_2	CH_2 of all amino acid
4	3.81-4.88	10	CH_2(2) CH (8)	CH_2-Glycine CH of 8 amino acid (Chiral)
5	6.85-7.21	4	CH (Aromatic)	Tyrosine
	Total	50		
Remark: -		Solvent peak observed: - 1.96-2.01ppm (Acetic acid),		
		No peak for -OH/NH_2/NH observed in spectrograph as it is an exchangeable proton. (Total = 16H)		

Table 6.4 summarised number of protons observed in NMR spectra for oxytocin (Figure 6.3). Twelve number of proton signal was found to be between 0.98-0.99 that represents the proton present in primary aliphatic carbon which confirms Isoleucine/leucine amino acid Table 6.4. Similarly, chemical shift from 1.19 to 1.61, 1.62-3.77 represents number of protons present in aliphatic tertiary and secondary carbon respectively. Hence, 2 protons in tertiary and 22 in secondary carbon confirm the presence of Isoleucine/Leucine and CH_2 for all amino acid respectively. Chemical shift from 3.81 to 4.88 represent 8 protons present in chiral carbon, and 6.85 to 7.21 represent 4 protons present in chiral carbon of tyrosine. Overall, the presence of protons confirms structure of amino acids in oxytocin 2-(2-(2-Aminoethoxy) ethoxy) acetic acid. Additional number of proton presence (Figure 6.4 & Table 6.4 & 6.5) in AEEA-Oxytocin was further concluded for particular amino acid or its alignment with particular group confirmed by NMR spectra.

Table 6.5: Observations from NMR spectra of AEEA-Oxytocin

S. No.	Chemical Shift ppm	No. of Proton	Assignment of Proton	Remarks
1	0.87-0.95	12	CH_3	Isoleucine/Leucine
2	1.09-1.32	2	CH	Isoleucine/Leucine
3	1.26-3.77	32	CH_2	AEEA and CH_2 of all amino acid
4	3.83-4.83	10	CH_2(1) CH (8)	CH_2-Glycine CH of 8 amino acid (Chiral)
5	6.78-7.15	4	CH (Aromatic)	Tyrosine
	Total	60		
Remark: -		Solvent peak observed: - 1.97-2.01ppm (Acetic acid),		
		No peak for -OH/NH_2/NH observed in spectrograph as it is an exchangeable proton. (Total = 17H)		

2-(2-(2-Aminoethoxy) ethoxy) acetic acid was successfully conjugated with oxytocin and further confirmed by Mass spectroscopy. The total mass of AEEA-Oxytocin is 1151.509 that confirms the conjugation of oxytocin with AEEA in direct HR-Mass (Figure 6.6).

Table 6.6: Major Peaks observed in MS spectra

m/z	Rel. Abundance, %	Fragment
1151.509 [Mono isotopic mass]	100.00	$[C_{49}H_{77}N_{13}O_{15}S_2]^+$

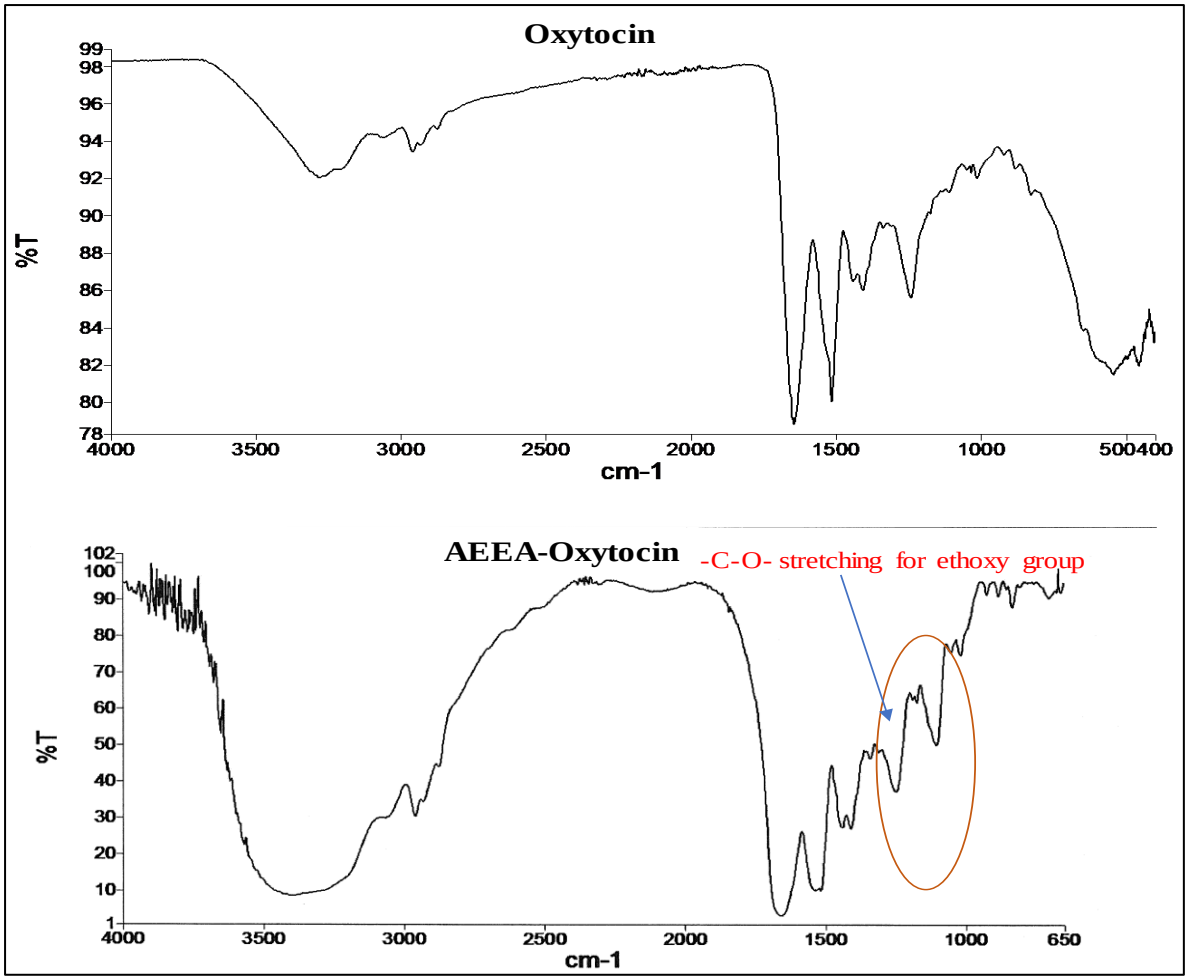

Figure 6.3: FT-IR Spectra of AEEA-Oxytocin

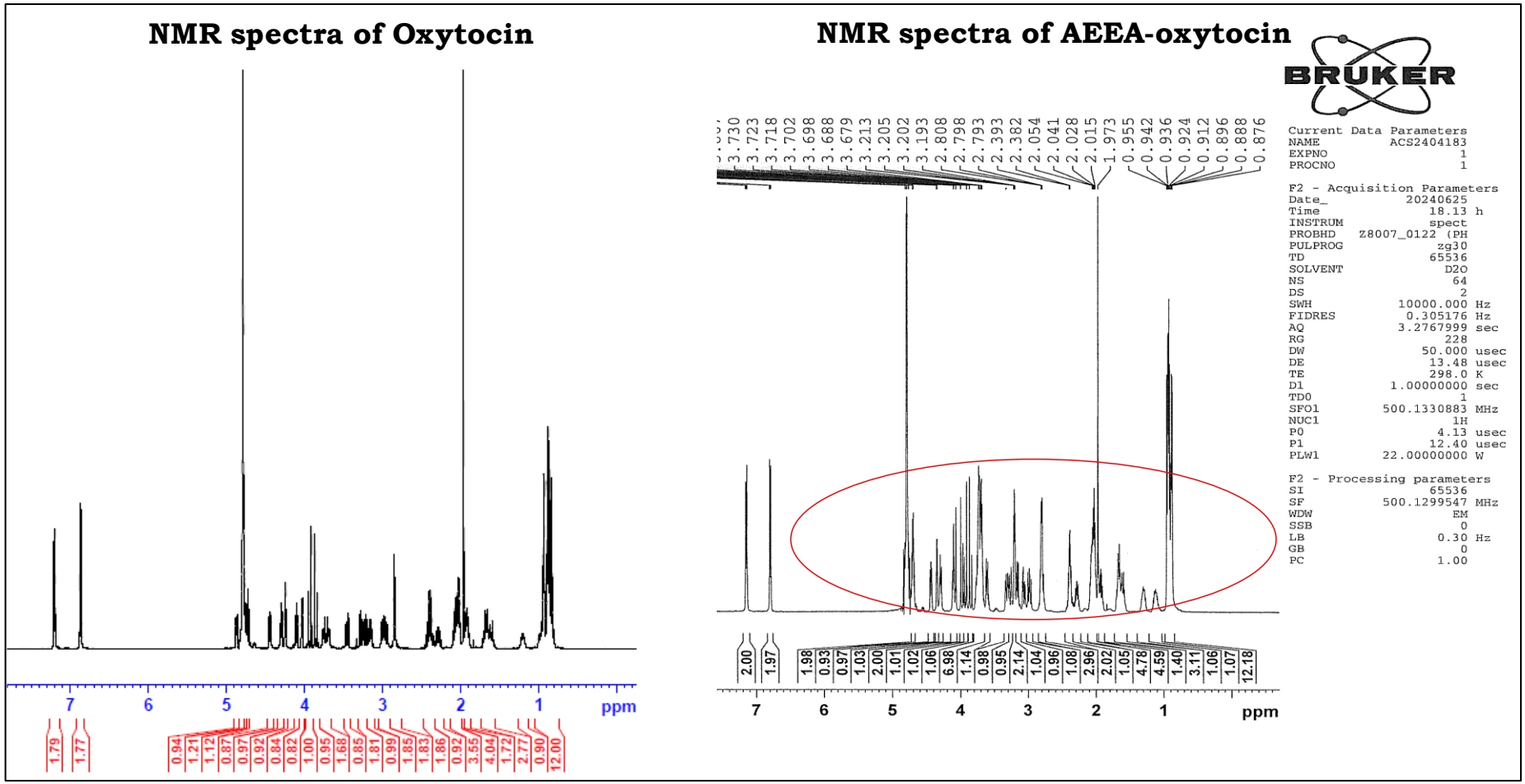

Figure 6.4: NMR spectra of oxytocin & AEEA-Oxytocin

Oxytocin

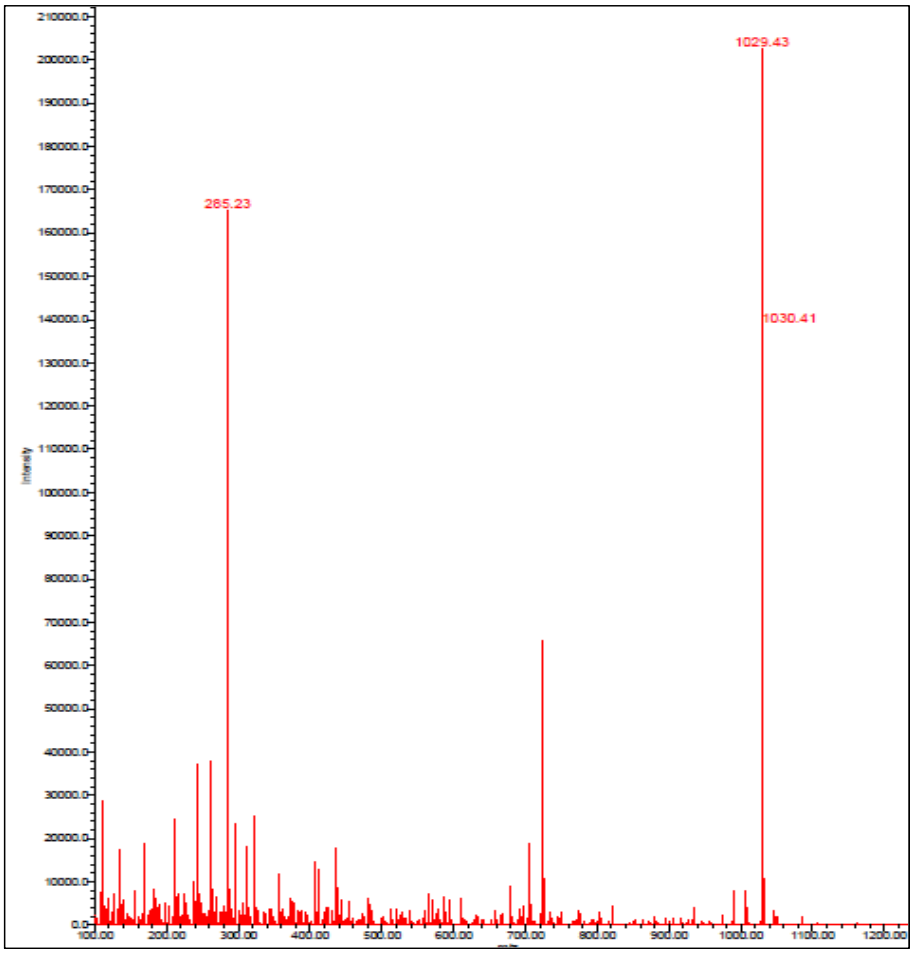

AEEA-Oxytocin

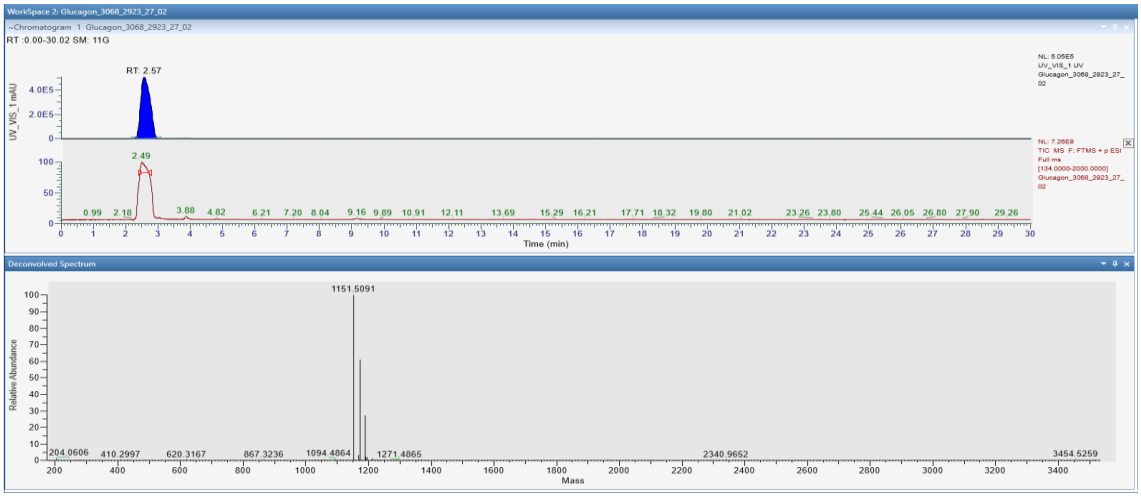

Figure 6.5: Mass spectra of Oxytocin and direct mass spectra of AEEA-oxytocin

6.6.2 *In vitro* cell line study

6.6.2.1 Evaluation on SH-SY5Y neuro cells

6.6.2.1.1 Cell viability and biocompatibility

The cell viability study was conducted in SH-SY5Y cells employing MTT assay to investigate the biocompatibility of Oxytocin and AEEA-oxytocin towards tested cells. Biocompatibility associated with Oxytocin and AEEA-oxytocin containing 1 µg/mL, 10 µg/mL and 100 µg/mL with subsequent incubation with SH-SY5Y neuro cells for 24, 48 and 72 h was calculated (Figure 6.6) [12]. It was observed that above 85% cell viability during increasing concentration at given time points (24 h, 48 h and 72 h) with OXT and AEEA-OXT. However, cell viability reduced from 95% to 85% after 72 hr exposure of formulation at higher concentration (100 µg/mL). The cell viability above 85% at all tested conditions suggest that OXT retained its biocompatibility on neuro cells even after being conjugated with AEEA. The conjugation of peptide with AEEA depicted similar pattern of neuro protective potential compared to that seen with plain OXT. In conclusion, no reduction of cell viability or more precisely cytotoxicity with increase in concentration at time points with both oxytocin and AEEA-OXT. The outcome of current study suggests that OXT and its conjugated counterpart are compatible with neuro cells at concentration of 100 µg/mL

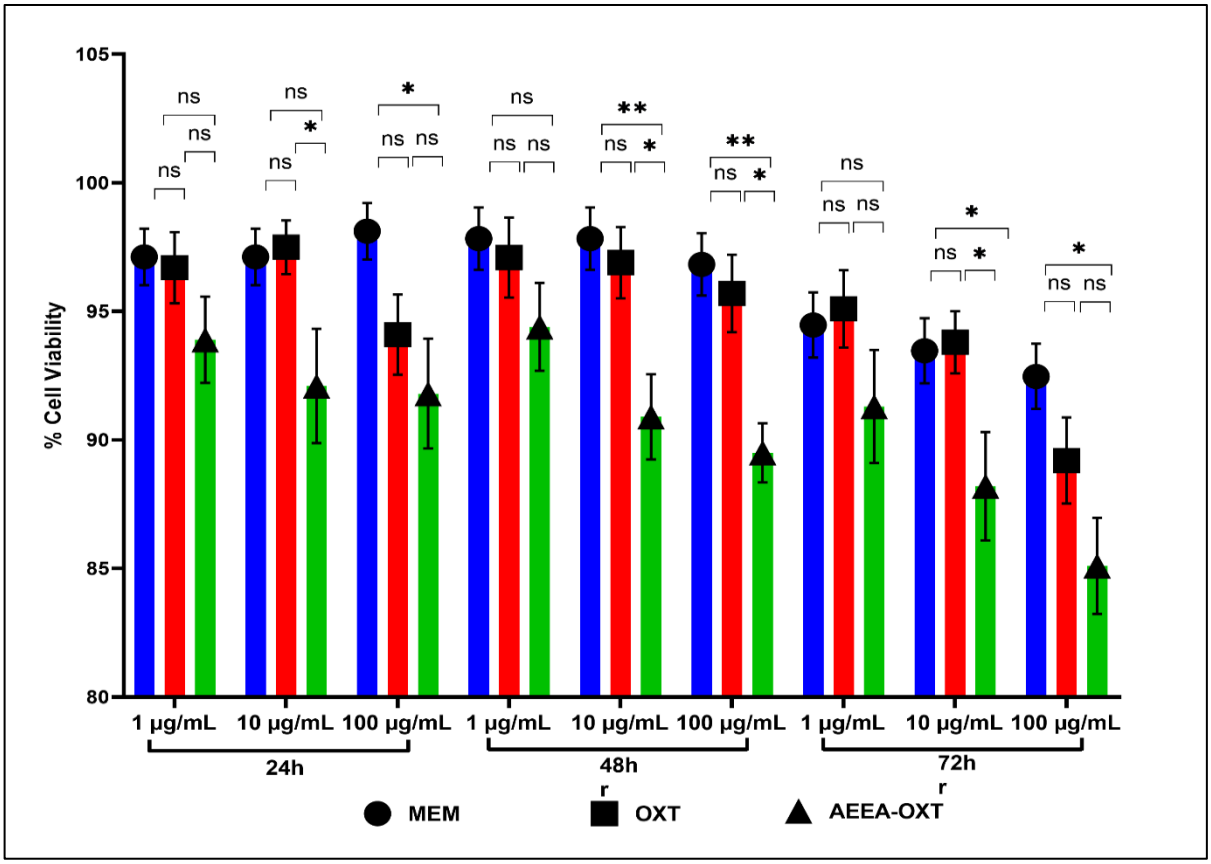

Figure 6.6: % Cell viability after the exposure of oxytocin and AEEA-oxytocin after 24 hr, 48 hr & 72 hr incubation.

6.6.2.1.2 *In vitro* cell uptake study: quantitative

The quantitative cell uptake study of OXT and AEEA-OXT was carried out in SH-SY5Y cells to determine internal localization proficiency. The data obtained from cell uptake evaluation study confirmed remarkably higher internal localisation of OXT and AEEA-OXT after 3 hr incubation (Figure 6.7). Maximum cell uptake was found to be at the highest concentration (0.4 mg/mL) that confirms the concentration dependent cellular uptake. The concentration dependent cellular uptake implicates that cells are more susceptible to allow conjugated OXT over Plain OXT. This might be due to availability of more N-terminal chain in conjugated OXT in comparison to free OXT. Time-dependent cellular internalization of OXT and AEEA-OXT was demonstrated in cell uptake investigation, and increases with increase in incubation period from 1 to 3 hours. This significantly enhanced the amount of OXT that was taken up by the cells. Significant changes in cell uptake with time was observed when incubation period

extended from 2 hours to 3 hours. In conclusion, time and concentration dependable cellular uptake was found for OXT and AEEA-OXT.

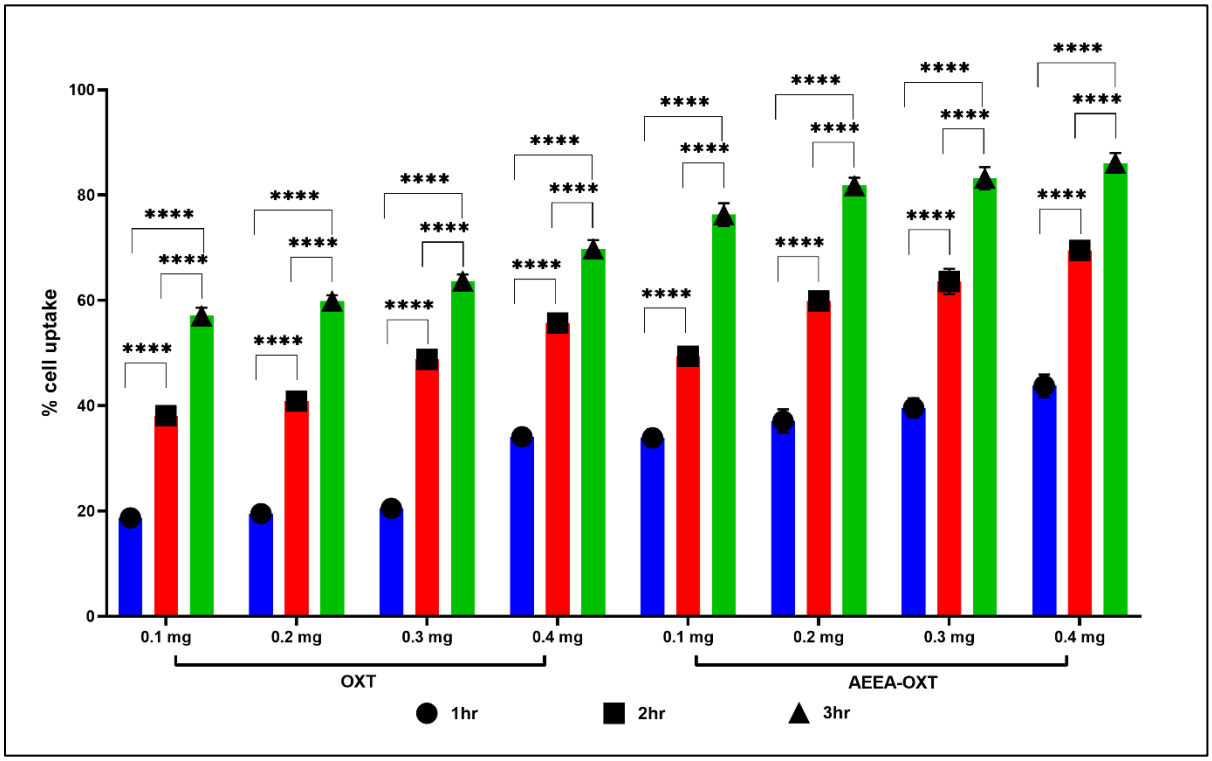

Figure 6.7: % of Cell uptake after the exposure of oxytocin and AEEA-oxytocin after 1 hr, 2 hr & 3 hr incubation (n=3).

6.6.2.1.3 Morphological observations

The effect of oxytocin and AEEA-Oxytocin on SH-SY5Y cells was evaluated by observing cellular morphology. After the treatment with pure OXT and its conjugation with AEEA (AEEA-OXT) for 48 hr, the morphology of cells remained same as control and not detected any changes compared to control under a phase contrast microscope (Figure 6.8). In SH-SY5Y cells treated with formulations, no visual changes of characteristic features of apoptosis, such as disruption of a cell wall, shrinkage of cell, and decrease in number of living cells, compared to control group was observed.

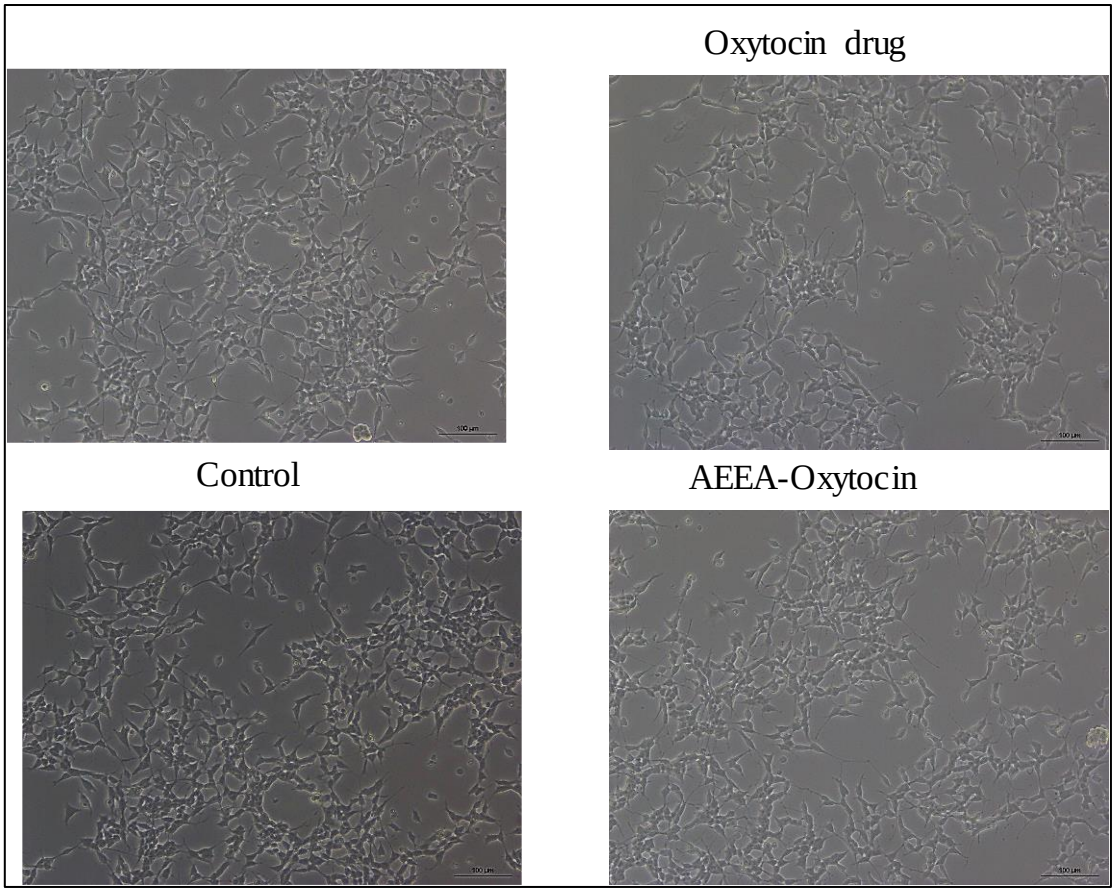

Figure 6.8: Morphological observation of SH-SY5Y cells treated with high dose (100 µg/mL) of oxytocin and AEEA-Oxytocin for 48 hr at 20X magnification.

6.6.2.1.4 *In vitro* cell permeation study (Cell uptake*)*

The comprehensive study examining cell uptake of C-6, C6+OXT and C-6+AEEA-OXT, was conducted using SH-SY5Y cells to evaluate effectiveness of conjugation in cellular internalization. The results from this meticulous cell uptake evaluation revealed a slightly higher internal localization of AEEA-OXT following an incubation period of three hours (Fig 6.9). These findings serve to support the hypothesis regarding cellular uptake of AEEA-OXT, as indicated by persistent and vibrant fluorescence signals detected after three hours of incubation with C-6 + AEEA- OXT.

6.6.2.1.5 ROS (DCFDA) assay

ROS levels were not very high after treatment with pure oxytocin and AEEA-OXT. This was shown by green fluorescence genesis, which caused due to reaction of ROS and fluorescent

DCF. Figure 6.10 shows cells, marked with DCFDA and treated with oxytocin and AEEA-Oxytocin at a concentration of 100 µg/mL. There was almost same fluorescent emission with 100 µg/mL concentration of formulation when compared to control cells. The mean ROS fluorescence intensity of obtained images were done with help of Image J software. The ROS analysis outcome suggest that OXT retained its biocompatibility on neuro cells even after being conjugated with oxytocin. The conjugation of Oxytocin with AEEA depicted the similar neuro protective potential when compared with plain OXT. This implicates that, qualitatively OXT and AEEA-OXT exhibit similar pattern or more precisely AEEA-OXT preserves neuro-protective nature equivalent to OXT even after conjugation with AEEA.

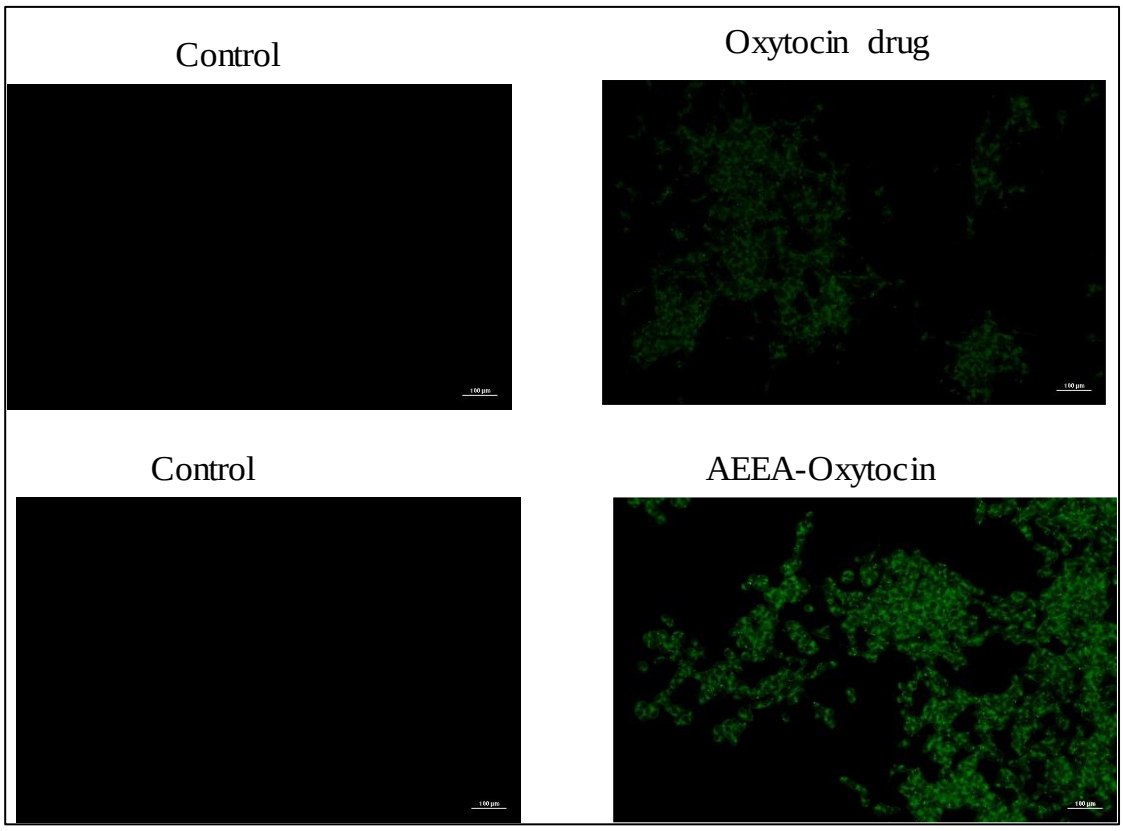

Figure 6.9: Cell uptake of SH-SY5Y cells control, treated with High dose (100 µg/mL) of oxytocin and AEEA-oxytocin for 48 hr at 20× magnification.

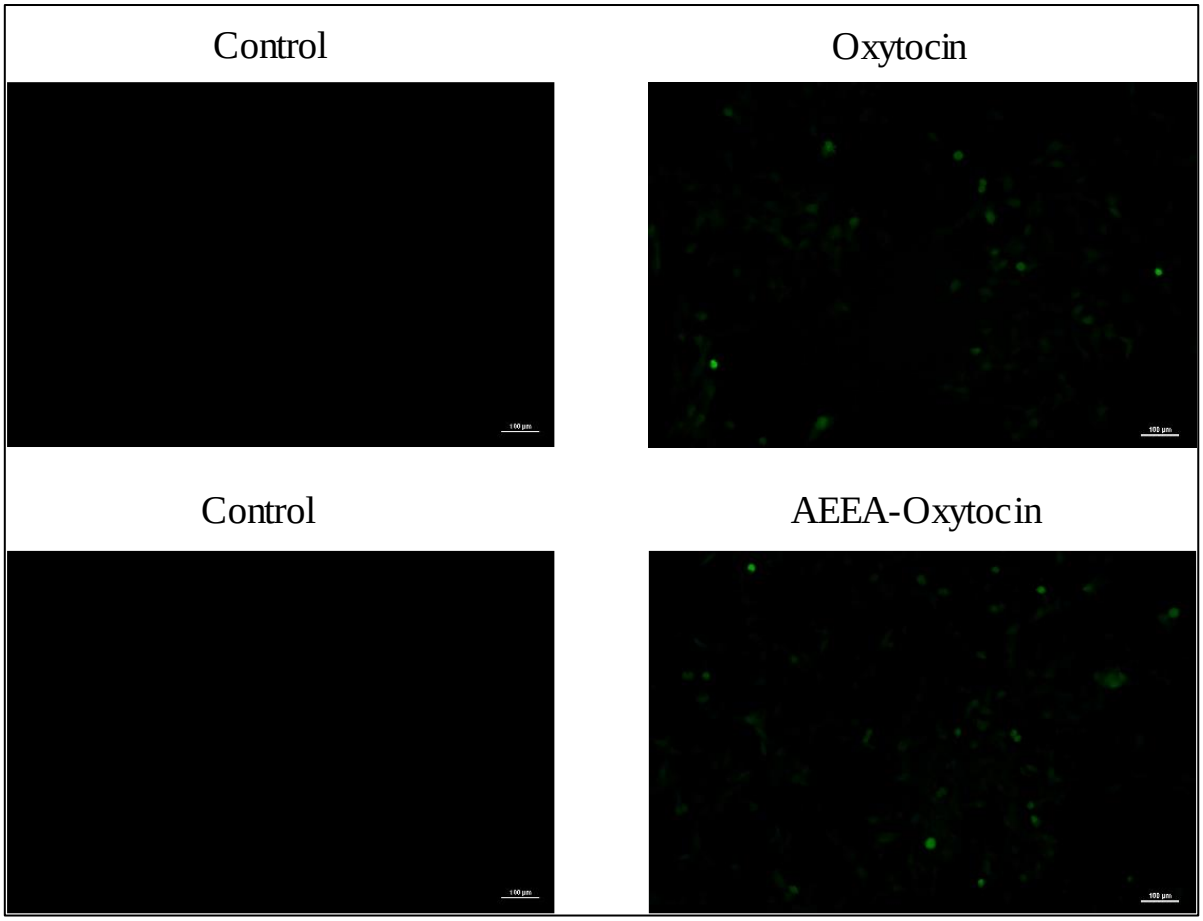

Figure 6.10: ROS generation of SH-SY5Y cells treated with control, oxytocin and AEEA-oxytocin at 100 µg/mL for 48 hr at 20X magnification.

6.6.2.1.6 Apoptosis assay (Qualitative cell study using AO/EB and DAPI staining)

The study of apoptosis in SH-SY5Y cells treated with Oxytocin and AEEA-Oxytocin was done by marking them with DAPI and a dual (AO/EB) method. Figure 6.11 shows normal SH-SY5Y cells with cell nuclei that remains as whole and marked with DAPI [28]. However, in SH-SY5Y cells treated with oxytocin and AEEA-Oxytocin, the nuclei did not show any morphological changes linked to apoptosis, such as nuclear condensation, increased brightness, or nuclear crinkle. This was confirmed by AO/EB staining. The cells in control group were live and transmitted off green fluorescence in a spherical shape. The nucleus was spread out evenly across the middle. No deformation in nucleus after treatment with OXT and AEEA-OXT depicts that both drugs do not show any toxic effect and they are safe as neurological therapeutics.

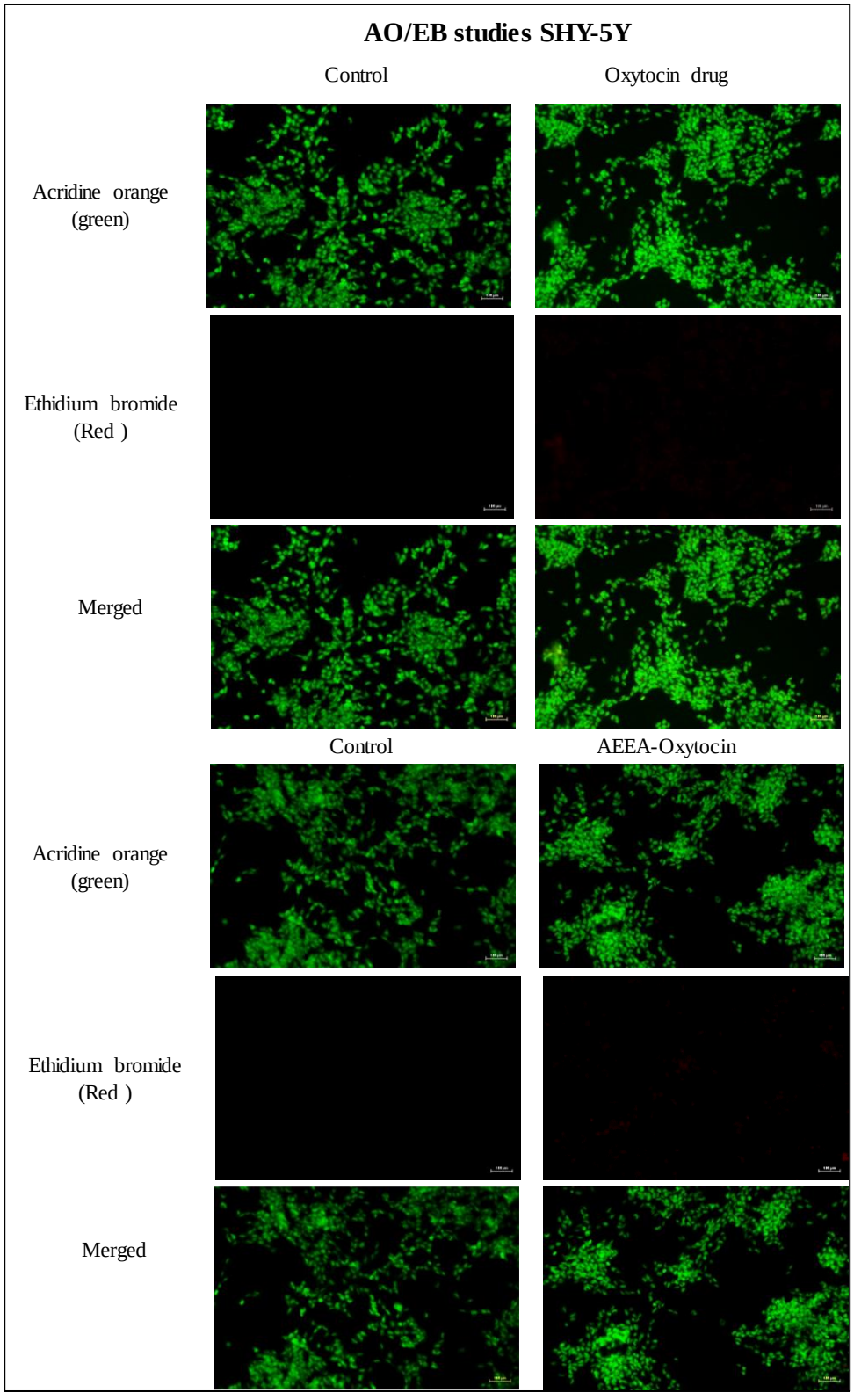

Figure 6.11: Acridine orange/Ethidium bromide dual staining studies of control, oxytocin and AEEA-oxytocin at high dose in SH-SY5Y cells for 48 hr at 20X magnification.

6.6.2.2 Evaluation on monocytic cells (THP-1)

6.6.2.2.1 Gene transcription analyses of inflammatory and apoptotic markers

The study was intended to assess effect of oxytocin and AEEA-Oxytocin on transcriptional pattern of inflammatory immune and apoptotic makers (NF-kβ, IL-6 Akt1, BCl, CD40, Bim, Bak, caspase-3, 8, 9). It was observed that there was decrease in caspase-3 and caspase-8 levels in hTHP-1 cells that were treated with oxytocin and AEEA-oxytocin (see Fig 6.12). Caspase-9 expression on contrary was seen higher with treated group. The expression levels of pro-apoptotic markers did not achieve statistical significance. It was noted that there was a decrease in expression of inflammatory markers NfKB and IL-6 in cells treated with all Oxytocin and AEEA-oxytocin. Remarkably, the co-stimulatory markers (CD40) that regulates programmed death and pro-apoptotic gene Bak was seen reduced with all formulations treated in hTHP-1 cells. However, Bim expression was seen higher by oxytocin formulation treated cells. Meanwhile, cell death and inflammation interlinked phenomena, relative to mRNA expression of IL-6 was determined. Oxytocin and AEEA-Oxytocin treated hTHP-1 cells showed a highly significant reduction in expression of pro-inflammatory marker, IL-6 as compared to control. The above studies indicated a down regulation of apoptotic and inflammatory markers after treatment with AEEA-OXT and OXT, implicating their neuroprotective role with promising safety and efficacy.

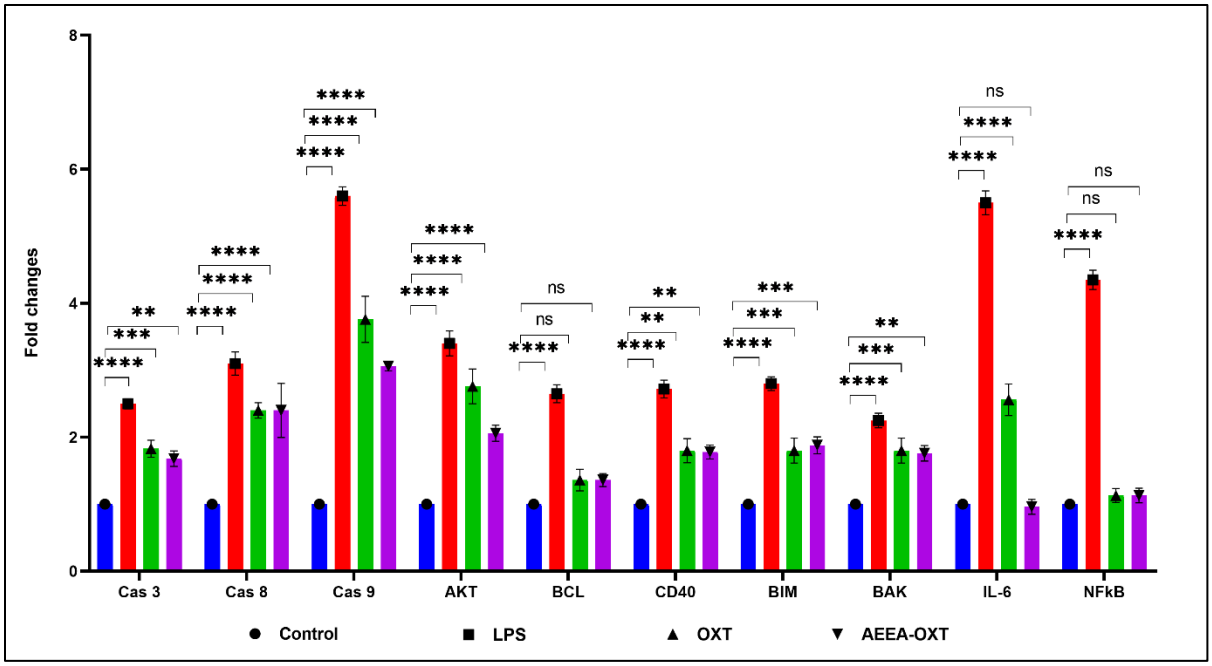

Figure 6.12: Determination of transcriptional gene expression of inflammatory, signalling and apoptotic markers.

6.6.2.2.2 Confocal microscopy-based immunofluorescence assay (IFA)

The objective of this study was to develop cell line model to find effect on FOXO1 after treatment with OXT and AEEA-OXT [24]. Following one hour of LPS stimulation, our results showed a significant difference in qualitative expression of FOXO1 when comparing LPS-stimulated cells to those that were unstimulated (Fig 6.13). Compared to unstimulated control, this study demonstrated in FOXO1 expression. Both OXT and AEEA-OXT showed better results compared to LPS stimulated cells. In conclusion, AEEA -Oxytocin showed better cell permeability in comparison to OXT due to presence of more N-terminal ends that aids in more internalization of conjugated OXT, leading to decrease in response of LPS stimulation and thus providing more effective treatment.

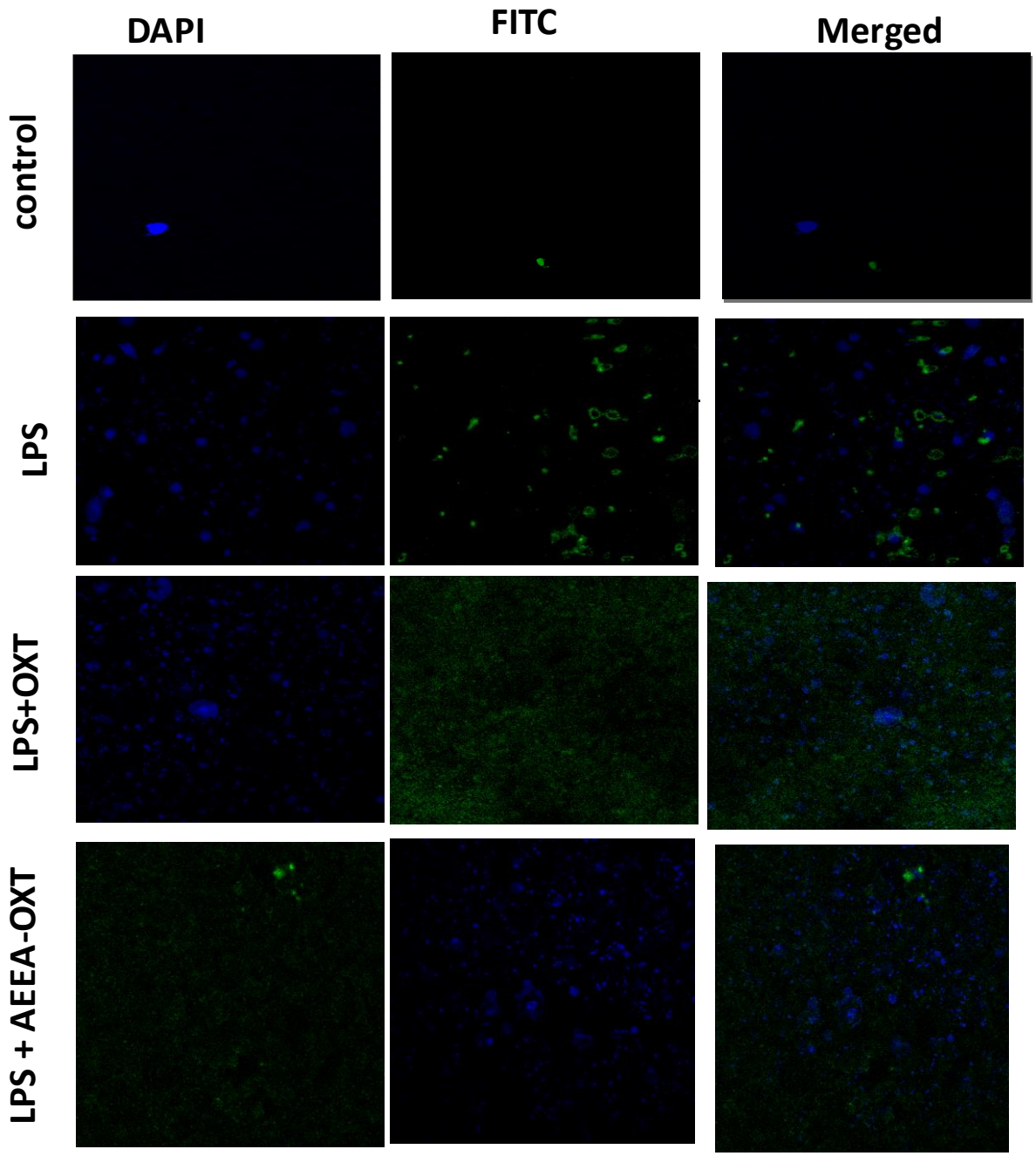

Figure 6.13: Expression of FOXO-1 gene following the LPS after various formulations treatment

6.6.3 Neurological effects in experimental animals

6.6.3.1 Morris water maze test

MWM test was evaluated by compare the free OXT and AEEA-oxytocin administered *via* IN route against positive control (Naïve) and negative control group (SCP only).

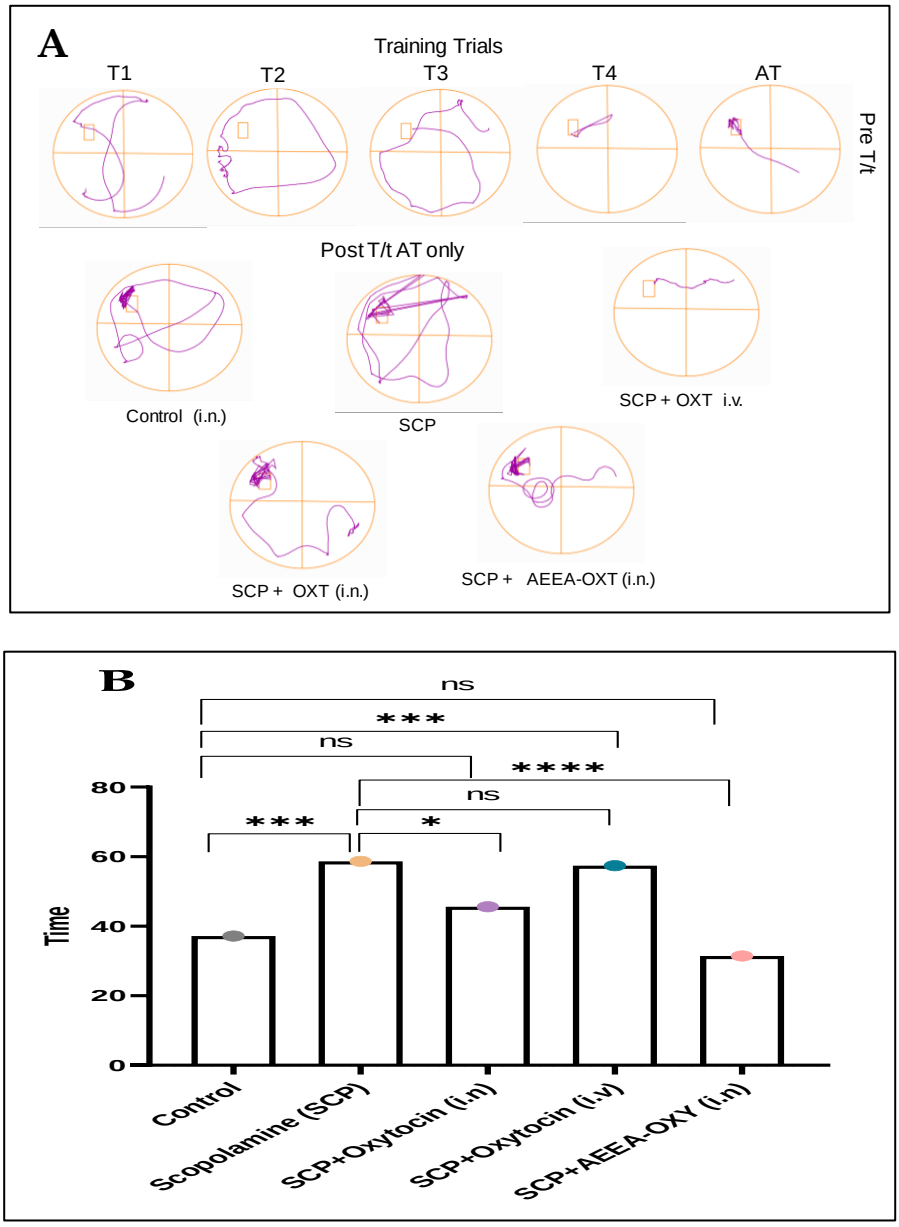

Figure 6.14: Pharmacological evaluations in Balb/C mice by MWM test: free OXT and AEEA-OXT administered intranasally. Data represents the control (Ctrl), scopolamine (SCP) treated, SCP + OXT (intranasal) and SCP + AEEA-OXT (intranasal). A) acquisition trials B) memory restoration by the OXT formulations treatmet. Time required in seconds by mice to reach the hidden platform.

For better understanding of safety and efficacy of proposed novel conjugate comparative cognitive functionality in animals' model of experimental AD was first studied. Morris water maze (MWM) test by administering OXT through IV and IN routes was compared with intranasally injected AEEA-OXT solution. AEEA-OXT solution was not studied via IV route in experimental mice model. Mice underwent a training protocol spanning four consecutive days, during which they were conditioned to navigate to a hidden platform located in the fourth quadrant of a standardized hidden maze. Upon completing this training regimen, a final acquisition trial was taken to assess the animals' ability to locate the hidden platform. Memory retention in the subjects was evaluated based on their latency to reach the target platform, as illustrated in Figure 6.14.

The comparison was made with naïve group of animals administered with placebo solution intranasally without any other treatment. The average mean time taken by mice to reach hidden platform was 37.16±6.75 seconds. However, average mean time taken by the mice with experimental memory deficit or SCP injected to reach the hidden platform was 58.66±1.18 seconds. This is 1.31 times to that of placebo/naïve control. We determined efficacy of OXT in mice when administered through IV and IN routes. SCP injected mice receiving IN treatment with OXT reached hidden platform in 39.58±4.45 seconds i.e., 1.07 and 0.67 times of placebo and SCP treated group respectively. Likewise, mice receiving IV treatment of OXT were seen to reach the hidden platform in 50.72±4.29 seconds i.e., 1.36 and 0.86 times of placebo and SCP treated group, respectively. Furthermore, the intranasally administered AEEA-OXT solution into mice were shown to reach the hidden platform in 26.45±4.23 seconds i.e., 0.72 and 0.45 times of placebo and SCP treated group. This investigation suggested that mice administered with AEEA-OXT solution took 0.66 and 0.52 times less time to reach the hidden platform when compared with the animals treated with plain OXT solution administered via IV and IN routes, respectively. The order for reaching hidden platform in quadrant 4 was AEEA-OXT (IN) < Naïve < OXT (IN) < OXT (IV) < SCP group respectively. These findings demonstrate the enhanced efficacy of AEEA-OXT solution administered intranasally. In this

study more emphasis was on time taken to reach hidden platform in quadrant IV. The earlier to reach hidden platform is directly proportional to memory retention of mice or specifically treated group. This study implies that memory of mice receiving treatment with AEEA-OXT through intranasal route not only regained but also improved as these treated mice reached the hidden platform quicker than the placebo control. This study demonstrates that intranasal administration of OXT effectively delivers the peptide to the brain, resulting in enhanced memory performance in animals compared to intravenous delivery. Notably, animals treated with AEEA-OXT via intranasal route exhibited superior memory retention compared to those receiving standard OXT intranasally, achieving the highest cognitive outcomes among both delivery routes. This enhanced memory might be due to more amount of OXT available in the brain when conjugated with AEEA and when administered via IN route. Apart from that, delayed or more time to reach hidden platform might be due to inadequate amount of OXT reaching the brain due to degradation when administered via IV route or IN. These neurobehavioral findings underscore the benefits of the intranasal route and the enhanced efficacy of AEEA-conjugated OXT over plain OXT.

6.6.3.2 Gene expression

Simple cognitive function studies were not enough to justify the efficacy of AEEA-OXT solution. For this, we have conducted gene expression studies to thoroughly understand the molecular fate of AEEA-OXT in mitigating neuronal markers. The conducted neurobehavioral studies indicated that intranasal administration of AEEA-OXT demonstrates superior efficacy compared to traditional OXT delivery methods, including both intranasal and intravenous routes. To further substantiate these findings, gene expression profiling of brain homogenates from the respective treatment groups were performed. Specifically, the gene expression analysis was conducted on brains isolated from animals undergone to Morris Water Maze (MWM) test. The evaluation focused on the expression levels of AIF-1, S100B, BDNF, and GFAP in brain homogenate samples derived from both OXT and AEEA-OXT treated animals.

The quantitative PCR from brain sample extracted from treatment groups to establish effectiveness of the OXT, AEEA-OXT. The transcription of following genes: AIF-1 (Allograft

inflammatory factor 1), known for its role in inducing inflammation; BDNF (brain-derived neurotrophic factor), a critical protein involved in the survival and growth of neurons; GFAP (glial fibrillary acidic protein), a marker of astrocytic activation; IL-6 (interleukin-6), an important cytokine involved in inflammatory responses; and Nrf 2 (nuclear factor erythroid 2-related factor 2), a vital regulator of antioxidant response. These genes are pivotal to understand the underlying molecular mechanisms that may be crucial in conferring the therapeutic effects of the treatment. AIF-1 derives from the neutrophils, macrophages, and microglial cells, has been a well-known neurodegenerative marker associated with calcium binding adaptor molecule-1. The efficiency of OXT-AEEA is marked by the expression of AIF-1. S100B is cytosolic calcium-binding protein, present in astrocyte, and secreted during the astroglial injury. Therefore, S100B gene expression studies to detect neuronal damage/neurodegeneration due to overly expressed in neuroglial cells. Eventually, these expression studies clearly suggested the prominent neutralization effect of intranasally administered conjugated-OXT. As GFAP is directly associated with the neuroinflammation, the brain tissue relative mRNA expression was seen similar to that with the untouched control (Figure 6.15). However, a many fold reduction in GFAP expression in the experimental (scopolamine treatment) AD was seen in group treated with intranasal AEEA-OXT. Whereas the intravenously and intranasally administered OXT reduced the GFAP expression but not to the extent as with the conjugated formulation.

The higher relative expression of BDNF, GFAP and S100b in AEEA-OXT administered through IN route and OXT given intranasally and intravenously treated group. A remarkable elevation in the expression of these markers was seen in the control (without AD) group. Whereas the experimental induced AD mice receiving intranasal treatment with the AEEA-OXT showed the increased expression of BDNF to that with the untouched control. Whereas BDNF expression was seen lower with other formulation and route of administration. More precisely, BDNF expression usually lower in AD patients in comparison to normal patients. Since the BDNF expression indicates the antioxidant and cholinergic transmission. Similar, pattern was observed in case of BDNF expression of AEEA-OXT and naïve mice brains. This means that AEEA-OXT is able to regulate BDNF expression in similar pattern to naive group. The pattern of BDNF expression was in order of AEEA-OXT (IN) = Naïve > OXT (IN) > OXT (IV) > SCP. The lower BDNF expression simulates to literature report of AD patients

and higher BDNF expression simulates to literature report of normal patients. BDNF expression of AEEA-OXT group also simulates to naïve group that clearly indicates the efficiency of route and conjugated system.

Increased GFAP levels were correlated with increased amyloid β levels and declined cognition. This GFAP is present in astrocytes. GFAP primarily marks its elevated expression both in serum and CSF of AD patients. The similar fashion was observed in our studies also. GFAP levels were in order of SCP > OXT (IV) > OXT (IN) > AEEA-OXT (IN) = naïve. The decreased expression in CSF of AEEA-OXT group and naïve group clearly indicates that IN route and conjugation of OXT with AEEA showed efficacy and similarity in pattern to naïve group. OXT administered via IV route in not efficient much to diminish the SCP treatment.

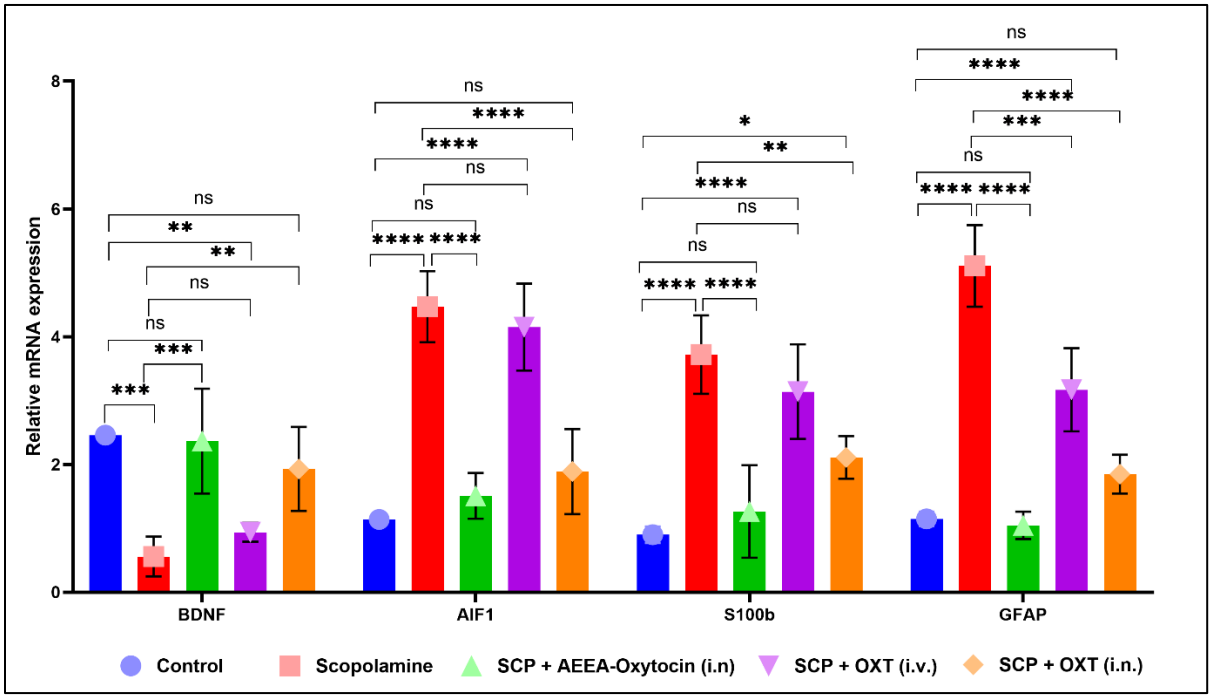

Figure 6.15: Gene expression of isolated brain. Data are represented for control (Ctrl), scopolamine treated (SCP), SCP + oxytocin (i.v), SCP + oxytocin (i.n) and SCP + AEEA-oxytocin (i.n).

S100b is a neuroprotective factor i.e., governed by neuroinflammation and its expression tends to upregulate in AD patients and it is expressed lower in normal patients. Similar pattern was observed in current research. The levels of S100b was found to be in order of SCP > OXT (IV) > OXT (IN) > AEEA-OXT (IN) > Naïve group. This order clearly signifies the efficacy of

conjugated OXT when administered via IN route. While OXT administered via IN route had higher expression this signifies diminished amount of OXT was delivered to brain and thus unable to treat.

AIF expression was correlated with neuronal cell death in cortex and hippocampal area of brain. The AIF expression was seen reduced with conjugated OXT administered intranasally similar to control. AIF expression was in order of SCP > OXT IV) > OXT (IN) > AEEA-OXT (IN) > Naïve. This is probably due to the protective sheath for OXT due to conjugation to protect OXT from physiological attacks of nasal environment and administration via IN route that clearly defines the efficacy of route and conjugation from above studies.

6.6.3.3 Biochemical estimations

Apart from gene expression and cognitive studies, biochemical parameters such as levels of antioxidant and production of free radical and lipid peroxidation to confirm the therapeutic role of OXT and AEEA-OXT and route of administration (Figure 6.16). In current scenario, MDA, nitrite activity, GSH and peroxide activity was studied.

MDA levels tends to rise in AD patients due to formation of peroxidation in brain and serum samples. MDA expression directly influences the oxidative stress in AD. Similarly, nitrite activity seems to be in similar fashion in AD patients as nitric oxide is one of the by-products. GSH expression is inversely proportion to oxidative stress. More GSH means patient is less prone to AD and lower the GSH patient is more prone to AD. H_2O_2 degrading activity is directly proportional to ROS. More the presence of H_2O_2 signifies the presence of oxidative stress due to inability of physiological system of brain to degrade it. And more accumulation leads to neuronal damage and neuroinflammation. The prepared brain homogenate from naïve, mice with experimental mice (by the SCP treatment), mice receiving free OXT through both intravenous and intranasal routes and intranasally treatment with AEEA-OXT were studied.

The SCP treatment showed higher secretion of MDA (lipid peroxidation biomarker), nitrite and peroxide activity levels and significantly comparative to naïve control group. However, OXT administered via IV route also showed the higher MDA, nitrite and peroxide activity levels in comparison to OXT administered via IN route in form of plain and AEEA-OXT. Conjugated AEEA-OXT upon IN administration reduced the MDA, nitrite and peroxide

activity levels similar to naïve control. Summarizing, levels of MDA, nitrite and peroxide activity were in order of: SCP > OXT (IV) > OXT (IN) > AEEA-OXT (IN) ≥ Naïve group.

The reduced levels in treated group signifies that, OXT administered in conjugation and via IN route is more effective to deduce AD related biochemical parameters. Apart from that conjugated OXT tends to be present in therapeutic concentrations in brain when compared to with plain OXT administered via both IN and IV route. The antioxidant GSH levels were in order of: SCP < OXT (IV) < OXT (IN) < AEEA-OXT (IN) < Naïve group. The higher level in conjugated OXT signifies that more OXT is able to reach in brain and tends to sustain in biological environment of brain in therapeutic levels. Apart from that, plain OXT injected through intravenous and intranasal route showed the protective effect by controlling GSH activity but not in significance to AEEA-OXT group.

The above cognitive, gene expression and biochemical studies revealed about conjugated OXT dominance in terms of efficacy over the plain OXT when delivered via IN route in SCP mice. This clearly establishes that OXT when administered in form of conjugation tends to sustain in brain for longer intervals when compared with plain and effectively delivered molecule at site of choice.

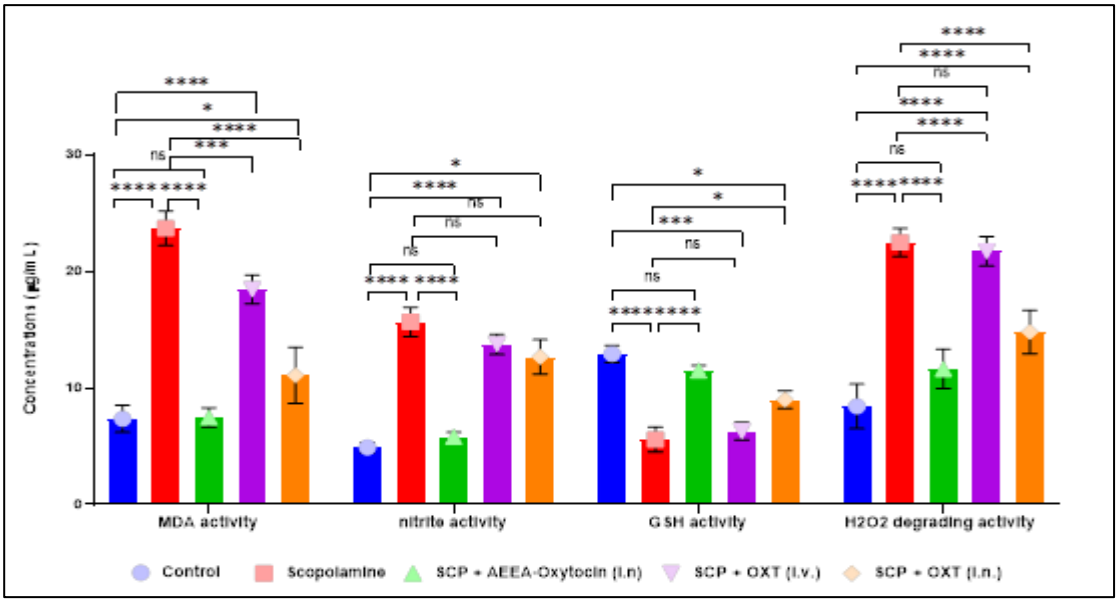

Figure 6.16: Biochemical estimation of homogenated brain. Data are represented for control (Ctrl), scopolamine treated (SCP), SCP + oxytocin (i.v), SCP + oxytocin (i.n) and SCP + AEEA-oxytocin (i.n).

6.6.3.4 Brain Histopathology examinations

The histological assessment of hippocampal observations indicates relative differences in effectiveness of formulation as suggested in present study. The density of neurons was found to be higher in naïve group followed by AEEA-Oxytocin delivered via Intranasal route, oxytocin delivered via Intranasal route, SCP treated group (Figure 6.17). The neuronal density is main functionality of human brain where it is directly proportional to effectiveness of treatment. So, in this study higher neuronal density was observed in group where no treatment was provided, followed by group treated with AEEA-OXT delivered via IN route. This implicates efficacy of conjugated OXT over the plain OXT.

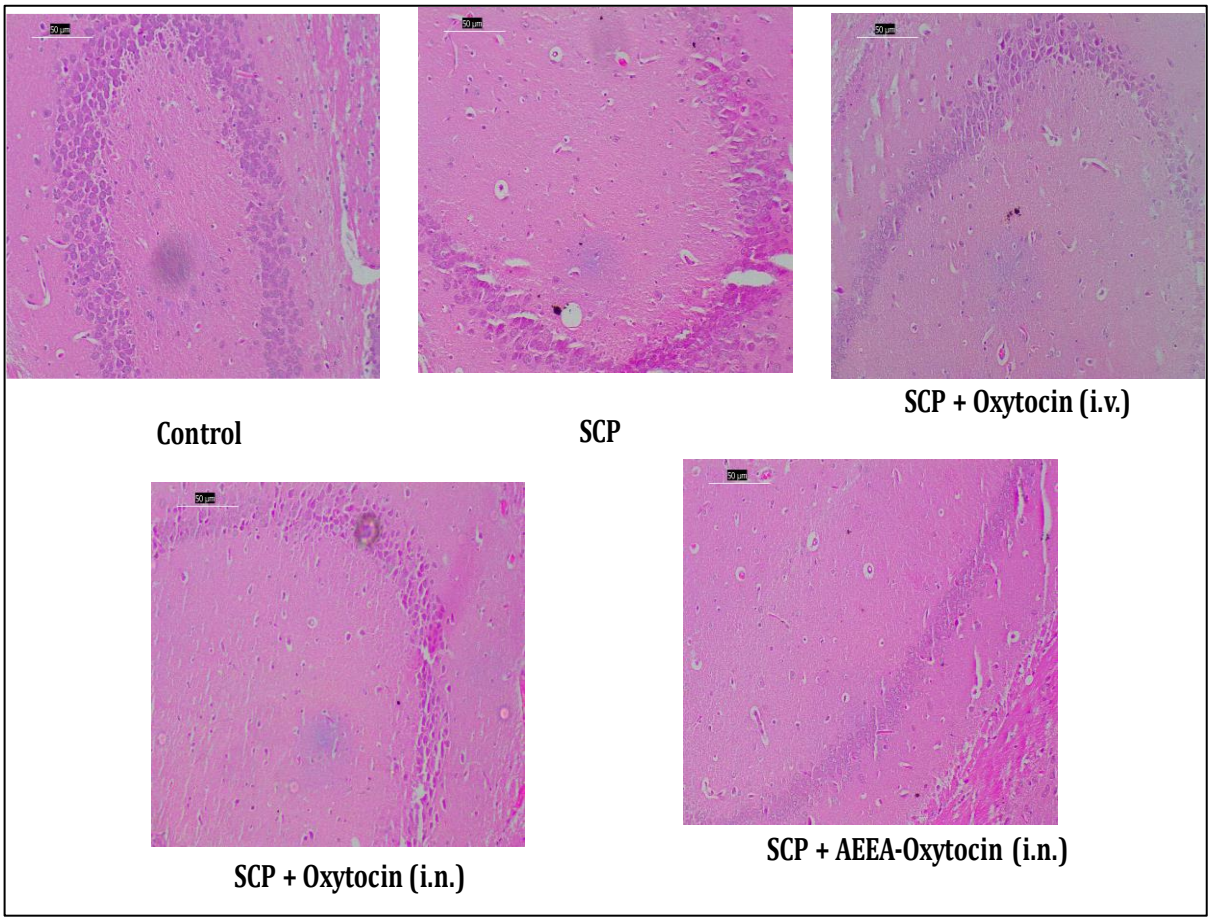

Figure 6.17: Images of histopathology evaluation of brain Hippocampus of Balb/C with scale 50 µm. Animals treated with free oxytocin and AEE-Oxytocin solution via i.n. route. Data are represented for control, scopolamine treated (SCP), SCP+OXT intranasal (i.v) SCP+OXT intranasal (i.n), SCP+AEEA-OXT (i.n.).

References

1. Kaneko Y, Pappas C, Tajiri N, Borlongan CV. Oxytocin modulates GABAAR subunits to confer neuroprotection in stroke in vitro. Scientific reports. 2016 Oct 21;6(1):35659.
2. Morales T. Recent findings on neuroprotection against excitotoxicity in the hippocampus of female rats. Journal of neuroendocrinology. 2011 Nov;23(11):994-1001.
3. Chilumuri A, Milton NG. The Role of Neurotransmitters in Protection against Amyloid-β Toxicity by KiSS-1 Overexpression in SH-SY5Y Neurons. International Scholarly Research Notices. 2013;2013(1):253210.
4. Handa M, Singh A, Bisht D, Kesharwani P, Shukla R. Potential of particle size less than 15 nm via olfactory region for direct brain delivery via intranasal route. Health Sciences Review. 2022 Sep 1;4:100038.
5. Pardridge WM. Drug transport across the blood–brain barrier. Journal of cerebral blood flow & metabolism. 2012 Nov;32(11):1959-72.
6. Trevino JT, Quispe RC, Khan F, Novak V. Non-invasive strategies for nose-to-brain drug delivery. Journal of clinical trials. 2020;10(7).
7. Di L. Strategic approaches to optimizing peptide ADME properties. The AAPS journal. 2015 Jan;17:134-43.
8. Monty OBC, Simmons N, Chamakuri S, Matzuk MM, Young DW . Solution-Phase Fmoc-Based Peptide Synthesis for DNA-Encoded Chemical Libraries: Reaction Conditions, Protecting Group Strategies, and Pitfalls. ACS Combinatorial ScienceVol 22/Issue 12. ACS Comb. Sci. 2020, 22, 12, 833–843
9. Baska F, Bozó É, Patócs T. Vasopressin receptor antagonists: a patent summary (2018-2022). Expert Opinion on Therapeutic Patents. 2023 May 4;33(5):385-95.
10. Garg NK, Tyagi RK, Singh B, Sharma G, Nirbhavane P, Kushwah V, Jain S, Katare OP. Nanostructured lipid carrier mediates effective delivery of methotrexate to induce apoptosis of rheumatoid arthritis via NF-κB and FOXO1. International journal of pharmaceutics. 2016 Feb 29;499(1-2):301-20.
11. Glavaš M, Gitlin-Domagalska A, Dębowski D, Ptaszyńska N, Łęgowska A, Rolka K. Vasopressin and its analogues: from natural hormones to multitasking peptides. International journal of molecular sciences. 2022 Mar 12;23(6):3068.

12. Neeraj K Garg NK, Singh B, Kushwah V, Tyagi RK, Sharma R, Jain S, Katare OP. The ligand (s) anchored lipobrid nanoconstruct mediated delivery of methotrexate: an effective approach in breast cancer therapeutics. Nanomedicine: Nanotechnology, Biology and Medicine. 2016/5/24 (12), 2043-2060.
13. Moroz E, Matoori S, Leroux JC. Oral delivery of macromolecular drugs: Where we are after almost 100 years of attempts. Advanced drug delivery reviews. 2016 Jun 1;101:108-21.
14. Amin SN, Younan SM, Youssef MF, Rashed LA, Mohamady I. A histological and functional study on hippocampal formation of normal and diabetic rats. F1000Research. 2013;2.
15. 14 Li Y, Li N, Yu X, Huang K, Zheng T, Cheng X, Zeng S, Liu X. Hematoxylin and eosin staining of intact tissues via delipidation and ultrasound. Scientific reports. 2018 Aug 16;8(1):12259.
16. Nie T, Wang W, Liu X, Wang Y, Li K, Song X, Zhang J, Yu L, He Z. Sustained release systems for delivery of therapeutic peptide/protein. Biomacromolecules. 2021 May 7;22(6):2299-324.
17. Zaman R, Islam RA, Ibnat N, Othman I, Zaini A, Lee CY, Chowdhury EH. Current strategies in extending half-lives of therapeutic proteins. Journal of controlled release. 2019 May 10;301:176-89.
18. Livak KJ, Schmittgen TD, Analysis of Relative Gene Expression Data Using Real-Time Quantitative PCR and the $2^{-\Delta\Delta CT}$ Method. Methods Volume 25, Issue 4, December 2001, Pages 402-408
19. Handa M, Sanap SN, Bhatta RB, Patil GP, Ghose S, Singh DP, Shukla R, Rahul Shukla. Simultaneous Intranasal Codelivery of Donepezil and Memantine in a Nanocolloidal Carrier: Optimization, Pharmacokinetics, and Pharmacodynamics Studies. Molecular Pharmaceutics. 2023 Jul 31;20(9):4714-28